Mapping of Local Field Potential Oscillations in the Rat Cerebellar Cortex Granule Cell Layer

Ettore Zuccheroso

A Thesis
in
The Department
of
Exercise Science

Presented in Partial Fulfillment of the Requirements
for the Degree of Master of Science (Exercise Science) at
Concordia University
Montreal, Quebec, Canada
August 2008

Your file Votre référence
ISBN: 978-0-494-45359-9
Our file Notre référence
ISBN: 978-0-494-45359-9

Abstract

Mapping of Local Field Potential Oscillations in the Rat Cerebellar Cortex Granule Cell Layer

Ettore Zuccheroso

Local field potential (LFP) oscillations in the granule cell layer of the cerebellar cortex could be a signal representing an organizing influence on its networks. However, little is known about the relative location of these LFP oscillations across the cerebellar cortex topography. LFPs and unit activity were recorded in the cerebellar cortex of 4 immobile adult male rats. Three to eight multiple moveable microelectrodes were simultaneously implanted at three targets (positions) perpendicular to the transverse plane. Recordings were made at regular 0.25 to 0.5 mm intervals, or upon a change in layers, or when capturing a single unit. LFPs were analyzed using Fast Fourier Transforms to calculate the proportion of the signal within 5-10 Hz for consecutive time windows of 500 ms. Recordings were made at multiple depths: for comparisons, track depth was divided in three regions (1/3 of the track depth, with region 1 being superficial and region 3 deep). All rats showed a tendency for increasing oscillatory activity with increasing depth and mean oscillatory activity increased from region 1 to region 3. Oscillatory activity was greater in electrodes located more lateral and caudal. All rats exhibited an interaction between position and region: increased oscillatory activity was found in lower depths of tracks more lateral and caudal, corresponding to position 1, region 3. 5-10 Hz oscillatory activity is isolated to specific subdivisions of the granule cell layer, corresponding to the

Crus II and paramedian lobules and could be related to the specific combinations of afferents arriving in these lobules.

Table of Contents

List of Figures

List of Tables

Introduction

Oscillations

This section will address oscillatory activity and its potential roles. The basic requirements for oscillations and their occurrence at different levels of organization will also be discussed. In addition, the generation of synchronous rhythmic activity and its role will be covered in this section.

Rhythmic Activity and Oscillations

The brain is a highly organized structure. Temporal information that is imperative for both motor behavior and cognition can be processed and generated by the brain (Buzsaki, 2006). This temporal information could be contained in oscillations that exist at many different time scales (Buzsaki, 2006). Oscillations have been thought to play an imperative role in coordinating the activity within and between systems in the brain and spinal cord on a temporal scale (Buzsaki & Draguhn, 2004; Gray, 1994). In addition, these neuronal rhythms occur in several distinct systems in the brain, over a wide range of frequencies and can be active during different states of behavior (Borisyuk & Kazanovich, 2006; Buzsaki, 2006; Gray, 1994). An oscillation is a rhythmic phenomenon characterized by a periodic variation in time of the recorded signal (Ermentrout, 2002; Wang & Rinzel, 1993). Oscillations can occur at the cellular level, both in the membrane and in the interactions between regions of a neuron, and in networks of neurons (Borisyuk & Kazanovich, 2006; Ermentrout, 2002). A prime example of oscillatory activity at the cellular level occurs in models of fast spiking neurons at rest that are injected with current and result in an increase in membrane potential due to the opening

of sodium channels (Ermentrout, 2002). Consequently, a slow outward potassium current is generated in addition to the inactivation and eventual closing of sodium channels at high potentials (Ermentrout, 2002). When a lower membrane potential is reached, sodium channels are not inactivated and potassium channels close so that the process can repeat itself (Ermentrout, 2002). In addition, several mechanisms such as single pacemaker neurons, through their membrane properties, and large cortical networks, by means of excitatory and inhibitory neuron interactions, can be responsible for rhythmic firing at different levels of organization (Ermentrout, 2002). A concrete example of neuron activity that oscillates is pyramidal cells in cortical layer 5 which exhibit intrinsic oscillations in the 5 – 12 Hz range and areas such as the pulvinar or the mesencephalic reticular formation can act to facilitate stimulus-specific synchronization in the cat visual cortex (Ritz & Sejnowski, 1997).

This oscillatory activity can be monitored using recordings of local field potentials (LFPs), general measurements of local electrical activity recorded by an extracellular electrode over a small area of the brain that reflect a change in synaptic activity and current flow (Bedard, Kroger, & Destexhe, 2004; Laurent, 2002; Nadasdy, 1998). Local electrical activity reflects a summed average of input signals on the dendrites and cell bodies of up to thousands of neurons in the vicinity of the recording electrode (Buzsaki, 2006).

Synchronous Rhythms

Rhythmicity facilitates synchrony across large systems (Buzsaki, 2006). However, rhythmicity is not analogous with synchrony; an oscillatory system can include neurons that have the same period, but they need not fire synchronously (Baker, Kilner, Pinches, & Lemon, 1999; Jedlicka & Backus, 2006). In addition, a synchronized group of neurons may be aperiodic (Jedlicka & Backus, 2006). Synchronous network oscillations may be induced by individual pacemaker cells, reciprocal inhibition between interneurons, recurrent excitation between excitatory cells, feedback loops between excitatory and inhibitory subpopulations and electrical synaptic communication (Jedlicka & Backus, 2006). Electrical coupling via gap junctions between neuronal dendrites and axons may act differently than chemical synapses but synergistically to promote neuronal synchrony (Jedlicka & Backus, 2006). Rhythmic synchronous firing usually evolves through the combination of pacemaker cells and large cortical networks (feedback loops) (Bear, 2001; Jedlicka & Backus, 2006). Synchronized neuronal population activity is involved in motor, sensory and cognitive brain functioning and pathogenesis of disorders (Ermentrout, 2002). Modularity in synchrony of complex spike firing and a shift from intrinsic burst-firing mode to a single-spiking mode with acetylcholine (Ach) or norepinephrine (NE) application has been shown to occur in the cerebellum and relay neurons of the thalamus respectively (Bear, 2001; Ozol & Hawkes, 1997). The concepts and importance of synchronized oscillatory activity in the cerebellar cortex will be discussed in a subsequent section.

Cerebellar anatomy and function

This section will give insight to the anatomy and physiology of the cerebellum at both the gross and cellular level. A detailed examination will be given to the anatomical divisions of the cerebellum and their functional circuits along with the cellular circuitry and synaptic connections. Microanatomical transverse and parasagittal zonal arrangements along with afferent input projection patterns will be discussed. The involvement of the cerebellum in non-motor tasks will also be addressed.

Gross Anatomy

The cerebellum is located in the posterior aspect of the brain just below the occipital lobes of the cerebrum. Approximately 10% of the skull volume is occupied by the cerebellum, however, it has approximately the same amount of cells as the rest of the brain combined (Buzsaki, 2006; Ito, 1984). The cerebellum is composed of the right and left cerebellar hemispheres that are separated by the vermis, each consisting of a lateral and intermediate part (Ghez, 1991). The cerebellum is divided into three lobes: the small anterior lobe, the much larger posterior lobe and the inferior flocculonodular lobe. The primary fissure separates the anterior and posterior lobes whereas the posterolateral fissure divides the posterior and flocculonodular lobes. The cerebellum is foliated and composed of 10 lobules at the vermis, numbered I to X from rostral to caudal (Voogd, 1991). The lobules of the hemisphere are an extension of the lobules of the vermis and have a specific nomenclature (Voogd & Glickstein, 1998). The anterior and posterior lobes are composed of the hemispheric extensions of lobules I to V and lobules VI to IX

respectively whereas the flocculonodular lobe is an extension of lobule X (Voogd & Glickstein, 1998). Figure 1A depicts the unfolded cerebellar surface of mammals along with lobular identification and nomenclature. Three pair of cerebellar nuclei are present deep within cerebellar white matter; from medial to lateral the nuclei are named fastigial, interpositus and dentate. Figure 1B depicts the posterior view of the cerebellum showing divisions of the outer cerebellar cortex, the 3 deep nuclei and the lobules at the vermis.

Neuronal Components

The cerebellum is composed of different neuronal elements: those in the superficial cortical layers and those in the deep cerebellar nuclei (Llinás, 2004). The outer portion of the cerebellum, the cortex, consists of three layers: the molecular, Purkinje and granule cell layers (Bower, 2002). The molecular layer is composed of basket and stellate cells. The Purkinje cell layer is composed of a row of Purkinje cells, the large output cells of the cerebellar cortex (Bower, 2002; Saab & Willis, 2003; Voogd, 2003). The Purkinje cell plays an indispensable role in cerebellar information processing because it is the only output of the cerebellum (Apps & Garwicz, 2005). The granule cell layer contains Golgi, granule, Lugaro and unipolar brush cells (Geurts, De Schutter, & Dieudonne, 2003; Llinás, 2004). Granule cell axons ascend to the molecular layer where they bifurcate to form parallel fibers (Bower, 2002).

Input and Output

Two types of afferent fibers enter the cerebellar cortex: mossy and climbing fibers (Llinás, 2004). Mossy fibers are the major afferent input to the cerebellum and there are

many sources of this pathway, the largest of which is the cortex, which sends input to the cerebellum via the pontocerebellar pathway (Llinás, 2004). Other contributors include the vestibular nerve and nuclei, the spinal cord, the reticular formation, and feedback from cerebellar nuclei (Llinás, 2004). Climbing fiber projections arising from the inferior olive in the brainstem synapse on dendrites of Purkinje cells (Saab & Willis, 2003). Each climbing fiber contacts only one Purkinje neuron with multiple contacts (Buzsaki, 2006; Llinás, 2004). As the main Purkinje cell axon leaves the cortex, it gives off recurrent collaterals that ascend back through the granular layer to form plexi above and below the Purkinje cell soma and form synapses with Golgi and basket cells (Llinás, 2004). Purkinje cell axons also project to the cerebellar nuclei. Figures 1C and 1D show the 10 lobules at the vermis in the sagittal plane and different neuronal types and connections in the cerebellar cortex respectively (Llinás, 2004).

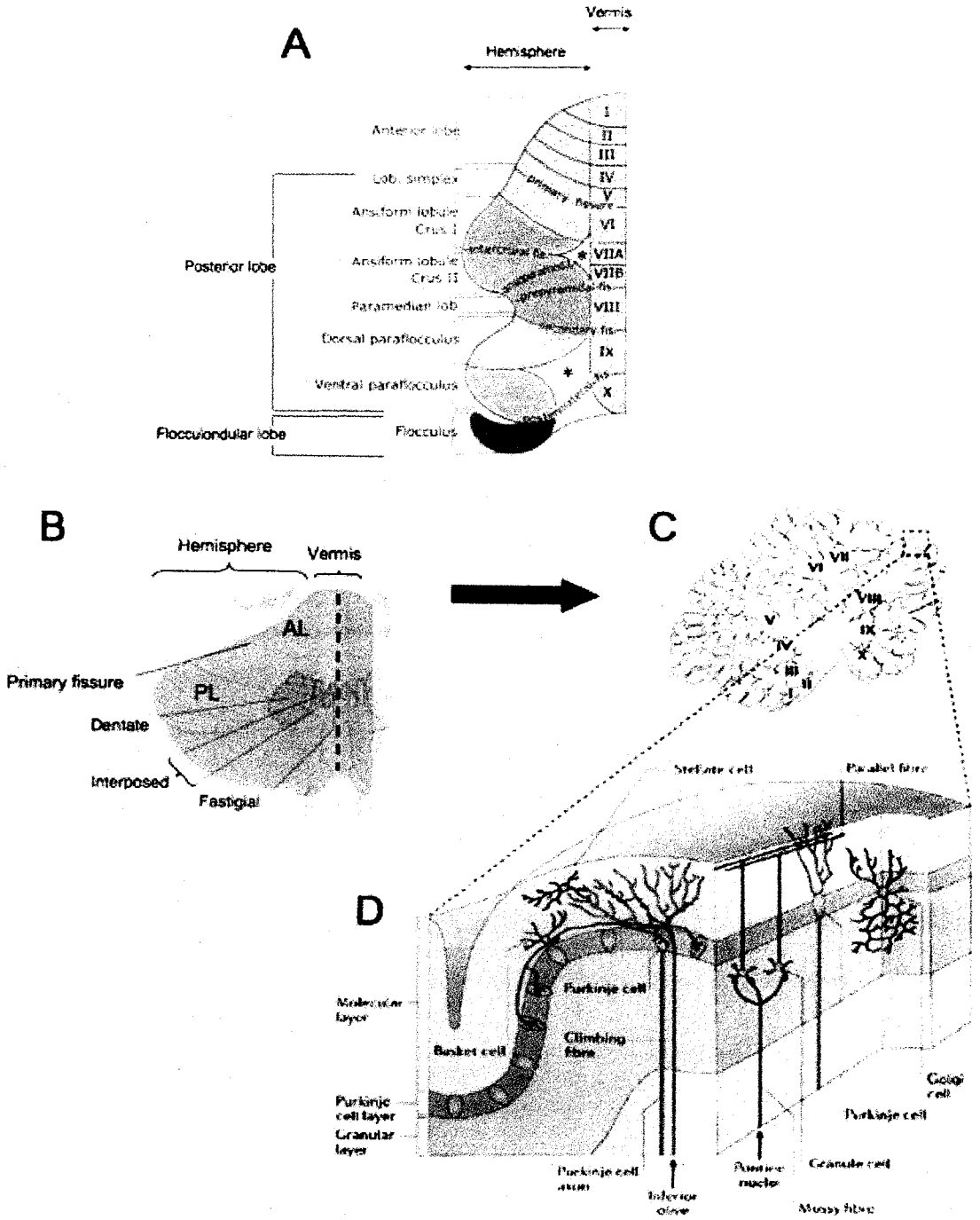

Figure 1

Anatomy of the Cerebellum

A. Schematic representation of unfolded cerebellar surface of mammals with lobular identification and nomenclature. **B.** Posterior view of cerebellum showing anterior and posterior lobes (AL and PL respectively) and the deep cerebellar nuclei. **C.** Mid-sagittal cross section through cerebellum. **D.** The cellular organization of the cerebellar cortex. Adapted and modified from Voogd & Glickstein, 1998 (A) and Ramnani, 2006 (B-D).

Synaptic Connections

The following section will describe the many excitatory and inhibitory connections and afferent input of the cerebellar cortex. In addition, some functional anatomy of cell types will be presented.

Inputs from mossy fibers make excitatory connections with granule, Golgi and unipolar brush cells whereas climbing fibers make excitatory connections with Purkinje cells (Geurts et al., 2003; Llinás, 2004). Mossy fiber afferents excite Purkinje cells indirectly through the granule cell-parallel fiber pathway causing them to discharge simple spikes (Apps & Garwicz, 2005). Climbing fiber connections with Purkinje cells generate complex spikes, the largest depolorizing event in any neuron (Apps & Garwicz, 2005).

Golgi cells receive glutamatergic excitatory connections from parallel fibers and their axons ramify extensively throughout the granular layer making GABAergic/glycinergic inhibitory contacts with granule and unipolar brush cells (Geurts et al., 2003; Llinás, 2004; Saab & Willis, 2003). Glutamatergic unipolar brush cells contact granule and other unipolar brush cells (Geurts et al., 2003). Unipolar brush cells act as a powerful feed-forward amplification system resulting in excitation of a large proportion of granule and unipolar brush cells through mossy fiber input (Geurts et al., 2003).

Lugaro cells are inhibitory interneurons that have their axonal plexi oriented in the parasagittal plane, contacting basket/stellate cells, or transverse plane contacting Golgi cells (Geurts et al., 2003). The transversal partly myelinated fibers in the molecular layer, oriented in a similar way as the parallel fibers, represent a source of transverse information flow in the cerebellum (Geurts et al., 2003). GABAergic Purkinje cells input onto Lugaro cells facilitating an inhibitory feedback circuit (Geurts et al., 2003). However, volume transmission provides Lugaro cells with excitatory input through serotonergic modulation (Geurts et al., 2003). Lugaro cells may be implicated in the synchronization of Golgi cells that run along the same parallel fiber and may organize granule cell layer oscillations (Geurts et al., 2003).

GABAergic basket and stellate cells of the molecular layer make inhibitory synapses on Purkinje cells (Llinás, 2004; Saab & Willis, 2003). Basket cells receive excitatory synaptic connections from climbing fibers and are inhibited by Purkinje cell axon collaterals. Parallel fibers make glutamatergic excitatory connections with dendrites of Purkinje cells, basket cells, stellate cells and Golgi cells (Saab & Willis, 2003).

Each Purkinje cell can receive input from up to 200 000 parallel fibers (Ramnani, 2006). The parallel fiber-Purkinje cell synapse has been implicated in cerebellar longterm depression (LTD), the weakening of the synapse that is believed to be involved in cerebellar motor learning (Ito, 2006). In order for LTD to occur at the parallel fiber-Purkinje cell synapse there must be co-activation of the climbing fiber synapse in the same Purkinje cell (Ito, 2006). An opposing mechanism to LTD is long term potentiation

(LTP) which occurs at the same synapse but does not necessarily require co-activation of the climbing fiber (Ito, 2006).

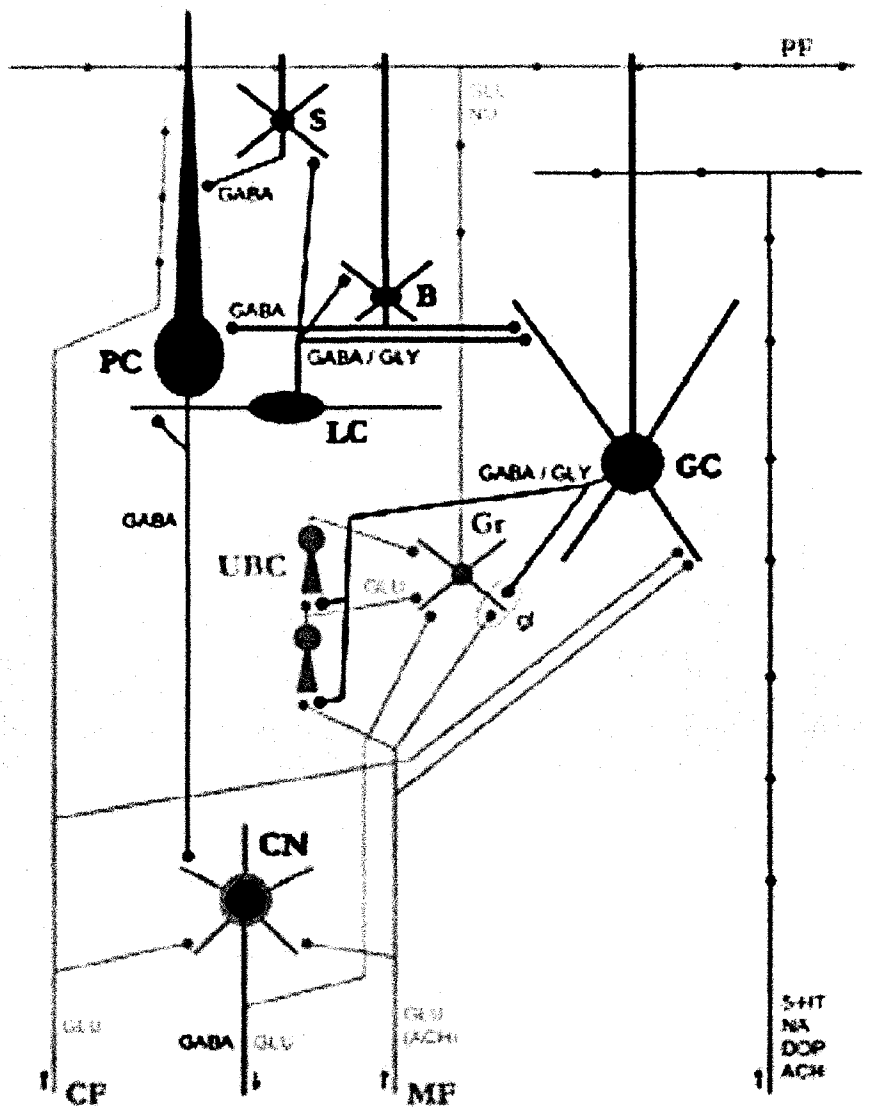

Figure 2

Synaptic Connections

Excitatory and inhibitory connections of different neuronal types and monoaminergic afferent input to the cerebellar cortex layer. Adapted from Guerts et al., 2003.

Monoaminergic Afferents and the Importance of Mossy Fiber Input

In addition to the inhibitory Golgi, basket, stellate and Purkinje cells, widespread modulatory effects can result from monoaminergic afferents. Constituents of all layers in the cerebellar cortex could be inhibited by norepinepherine via the superior cerebellar peduncle following activation of the locus coeruleus (Ghez, 1991; Ito, 1984). Dopaminergic cerebellar afferents project to the interpositus and lateral cerebellar nuclei and to the Purkinje and granule cell layers of the cortex (Ito, 1984). Serotonin exerts its effects on the cerebellar nuclei and the granular and molecular layers of the cortex via the projected afferents from the site of synthesis and release, the raphe nuclei (Ghez, 1991; Ito, 2006). The modulation of Lugaro cells by serotonin could provide the Golgi-granule cell network with resources for information patterning (Dieudonne & Dumoulin, 2000).

Mossy fiber afferents arise from several distinct sources such as diverse brain stem nuclei and from neurons in the spinal cord that give rise to the spinocerebellar tracts (Ghez, 1991). However, the major source of mossy fiber afferent input to the cerebellum comes from the cortex via the pontocerebellar pathway (Llinás, 2004). Clusters of granule cells are activated in response to activation of the mossy fiber pathway by peripheral stimuli (Ghez, 1991). In addition, mossy fiber projections indirectly excite Purkinje cells through synapses with granule cells (Ghez, 1991). In the cerebellum, mossy fibers terminate in patterns that are lobule-specific patches; pontocerebellar fibers terminate in the apex of all lobules, spinocerebellar fibers terminate as a layer just below and there is a concentric distribution of vestibular fiber projections terminating in the

base of the fissures at the vermis and slightly lateral (Glickstein, 2000; Voogd & Glickstein, 1998).

Cerebellar Unit Relation with Sensorimotor Processing

The cerebellar cell types and afferents mentioned previously are all involved to some degree with sensorimotor processing. While the thesis focuses on oscillations, a major modulating factor for cell activity, the following section will give insight to the cerebellar units' relationship with respect to movement and sensation. In addition, certain influences from the circuit organization are evident from the recordings in awake behaving animals. The circuit orientation and climbing fiber afferents will be presented here.

Excitatory and inhibitory input in the cerebellar cortex occurs in distinct planes; excitation to neurons along the mediolateral axis and inhibition to neurons along the anterior–posterior axis is termed "parallel fiber on-beam" and "parallel fiber off-beam" respectively (Heck, Thach, & Keating, 2007). Recordings of on-beam pairs of Purkinje cells in the cortex of awake behaving rats show that simple spikes are correlated in time, however, off-beam Purkinje cell pairs are not (Heck et al., 2007). In addition, synchronized on-beam activity is time locked to certain phases of the reaching and grasping movement (Heck et al., 2007). The movement related on-beam synchrony could represent temporal correlations of mossy fiber inputs via granule cell axons. Off-beam asynchronous activity may be a result of inhibitory interneurons that receive the same mossy fiber input but project in the off-beam direction only. In short, these observations implicate the cerebellum in timing and coordinating movement. In addition to afferent

input, Lu et al. (2005) showed that the timing of Purkinje cell simple spikes is greatly affected by activity in the underlying granule cell layer. Granule cell layer burst activity enhances simple spike activity in the majority of cases, however, inhibition of simple spikes did occur (Lu, Hartmann, & Bower, 2005). These results provide additional evidence that the synapses associated with the ascending segment of the granule cell axon have a substantial influence on Purkinje cell output. Also, since ascending granule cell axons make direct excitatory connections to inhibitory neurons in the molecular layer, reduction of Purkinje cell spike frequency occurs (Lu et al., 2005).

In addition to mossy fibers, climbing fibers are also implicated in sensorimotor processing. Cerebellar output may be altered temporally by the olivocerebellar system through synchronous sets of neuronal networks (Lang, Sugihara, Welsh, & Llinas, 1999). Recordings of complex spike activity from lobule Crus IIa in awake rats demonstrated that the olivocerebellar system generates synchrony among Purkinje cells located within parasagittally oriented strips of cortex and that many Purkinje cells display rhythmic complex spike activity at approximately 10 Hz (Lang et al., 1999). These parasagittal bands of synchronous complex spike activity may potentially contribute significantly to the motor output of the cerebellum, more precisely, having an organizing role in the timing of distinct muscle activation. In addition, it has been shown that input to the cerebellum from the inferior olive during skilled tongue movements in rats result in domains of Purkinje cell activity that are rhythmic and temporally related to movement (Welsh, Lang, Suglhara, & Llinas, 1995). These studies suggest that the inferior olive

organizes cerebellar output temporally and spatially via rhythmic firing and synchronously activating networks affecting muscle groups respectively.

Functional Circuits

In addition to the unit relation with sensorimotor processing, the cerebellum also functions on a larger scale in subdivided areas. The cerebellum is composed of three functional regions that have distinct anatomical connections with the brain: the vestibulocerebellar, spinocerebellar and cerebrocerebellar pathways (Ghez, 1991). It is by means of mossy fiber terminations to specific combinations of lobules and folia that the cerebellum is subdivided into functional regions (Voogd, 1991).

The vestibulocerebellar pathway consists of the flocculondular lobe that receives input from the vestibular nuclei in the medulla and projects directly back to them (Ghez, 1991; Voogd, Gerrits, & Ruigrok, 1996). The semicircular canals and the otolith organs are the major afferent inputs to the vestibulocerebellum (Ghez, 1991). This pathway is implicated in eye movements such as the vestibulo-ocular reflex (VOR) and is important for equilibrium and the control of the axial muscles that are used to maintain balance during stance and gait (Gomi & Kawato, 1992; Llinás, 2004). The VOR stabilizes retinal images by producing smooth eye movements that are equal and opposite to the rotary head movements during head turns (Gomi & Kawato, 1992). In addition, for the VOR to remain accurate it must be continuously recalibrated and this depends on the caudal cerebellar region (Glickstein, 2000). The spinocerebellar pathway consists of the vermis and paravermis regions that receive sensory information such as cutaneous and

proprioceptive information from the periphery, in particular from the spinal cord (Ghez, 1991). This pathway controls medial and lateral components of the descending motor systems and therefore plays a crucial role in controlling ongoing execution of limb movements (Ghez, 1991). Several mossy fiber pathways convey information from the spinal cord to the cerebellum; the dorsal and ventral spinocerebellar tracts act as direct pathways from the trunk and legs and the cuneo and rostral spinocerebellar tracts are the direct pathways from the arms and neck (Ghez, 1991). Projections from the vermis descend to the fastigial nuclei and this region of the cerebellum regulates axial and proximal musculature (Ghez, 1991). The intermediate part of the cerebellar hemisphere projects to the interposed nuclei and functions to promote distal motor control (Ghez, 1991). The cerebrocerebellar pathway receives input exclusively from the pontine nuclei that relay information from sensory and motor cortices and from premotor and posterior parietal cortices of the cerebral cortex (Ghez, 1991; Manto, 2006). The dentate nucleus relays output via the thalamus to the premotor, oculomotor, prefrontal and posterior parietal areas in addition to the motor cortex (Kelly & Strick, 2003; Llinás, 2004). The cerebrocerebellar pathway plays an intricate role in planning and initiation of movement. The lateral parts of the cerebellar hemispheres are implicated in fine dexterity tasks, attaining precision in the regulation of rapid limb movements and may also be implicated in general timing functions (Ghez, 1991).

Cerebellar Circuitry and Microanatomy

The cerebellum is compartmentalized into transverse zones and parasagittal strips that extend in the rostro-caudal and mediolateral planes respectively (Armstrong &

Hawkes, 2000). This compartmentation is due to the topography of cerebellar afferent terminals and chemoarchitecture of cell types (Armstrong & Hawkes, 2000). Four transverse zones have been identified in the cerebellum: the anterior zone (AZ, lobules I – V), the central zone (CZ, lobules VI, VII), the posterior zone (PZ, lobules VIII, IX) and the nodular zone (NZ, lobule X) (Armstrong & Hawkes, 2000). The four zones are differentiated through mutant strain lobulation characteristics and their gene expression patterns, such as zebrin I and II for Purkinje cells and acetylcholinesterase and acidic FGF1 receptor expression for granule cells (Armstrong & Hawkes, 2000). In addition to the zonal division of the cerebellum, the expression patterns of several antigens have identified parasagittal strips that subdivide the cerebellum mediolaterally in each zone (Armstrong & Hawkes, 2000; Herrup & Kuemerle, 1997). The cerebellar cortex is divided into alternating strips of zebrin II-immunopositive and zebrin II-immunonegative Purkinje cells in the AZ, PZ and hemispheres (Armstrong & Hawkes, 2000). The expression of molecular markers to subdivide the cerebellum into compartments is similar with the patterns of incoming afferents (Armstrong & Hawkes, 2000). Within each lobule there exists a diverse grouping of afferents that terminate and supply the cerebellar cortex with sensory and motor information (Sillitoe & Joyner, 2007). Climbing fiber afferents terminate in parasagittal bands that resemble Purkinje cell strips and mossy fibers project to parasagittal strips in the granular layer (Armstrong & Hawkes, 2000; Ozol & Hawkes, 1997). It has been shown by means of D-aspartate tracing, labeling of single olivocerebellar axons and cortical injections of cholera toxin B unit that most climbing fibers branch to narrow longitudinal bands in the cerebellar cortex in lobules VI and VII (Voogd, 1991). In essence, this distinct distribution results in an abundance of

climbing fibers to superficial depths of the cerebellum and a lack of these projections to deeper areas. In addition, the motor cortex sends projections to vermal lobules V and VI and hemispheric extensions of lobules VIIB and VIII whereas the prefrontal cortex connects mostly to lateral Crus II and vermal lobules VII and IX (Ramnani, 2006).

Cerebellar Functions and New Perspectives

Functionally, the cerebellum influences motor behavior, comparing actual motor output to what was intended and adjusting the movement as needed (Ghez, 1991; Saab & Willis, 2003). In addition, the cerebellum is implicated in the coordination of skilled movement, motor timing, eye movements and the control of motor tone, posture and gait (Salman, 2002). However, recent evidence suggests that the cerebellum is also implicated in non-motor tasks (Bellebaum & Daum, 2007; Salman, 2002). Based on neuroimaging and neurobehavioral studies, the cerebellum is now thought to be involved in sensory discrimination, attention, memory, verbal learning and complex problem solving (Allen, Buxton, Wong, & Courchesne, 1997; Bellebaum & Daum, 2007; Salman, 2002). The ability to learn music is affected in patients with cerebellar lesions being characterized by an increased variability in motor timing and a loss of auditory interval discrimination (Gordon, 2007). Lesions to the cerebellum do not always result in an ataxic condition, but rather cerebellar cognitive affective syndrome may develop (Gordon, 2007). This syndrome is believed to result from damage within a cerebocerebellar system and is characterized by impairements in executive functions, visual-spatial organization, verbal fluency and personality changes (Gordon, 2007). A consistent finding in neuroimaging studies is the recurrent activation of the Crus II region in cerebellar cortex during a verbal

working memory task (Ramnani, 2006). The cerebellum is connected through several intricate pathways with the cerebrum, basal ganglia, limbic system, brainstem and spinal cord (Salman, 2002). In addition, an electrophysiological study conducted by Crispino and Bullock (1984) showed evidence of the cerebellum modulating somatosensory, visual and auditory afferent sensory input to the midbrain, thalamus and cerebral cortex (Kern, 2002). Middleton and Strick (2001), showed that the cerebellum, in addition to projecting to multiple areas of the cerebral cortex via the thalamus, influenced several areas of the prefrontal cortex important for cognition. It is proposed that the cerebellum contributes both to motor control and cognitive functions because of its role in timing (Gordon, 2007).

Oscillatory activity in the cerebellum and local field potentials

This section will review aspects of rhythmic activity in the cerebellum of both rats and primates. The importance of climbing fiber input to the cerebellum will also be discussed. In addition, neurochemical circuits and their effect on field potentials and significant results from in vitro studies will be addressed. Lastly, the importance of mapping cerebellar granule cell layer oscillations is discussed.

Cerebellar Oscillations in Mammals

The cerebellum shows rhythmic behavior at both low and high frequency ranges (De Zeeuw, Hoebeek, & Schonewille, 2008). Purkinje cell complex spike activities occur at lower frequencies in the delta and theta range (2-10 Hz) and granule cell activity occurs within the theta range of 4-9 Hz in rats (De Zeeuw et al., 2008). Oscillations occurring at frequencies of 10-30 Hz (beta range) in primates are thought to be a result of the granule and Golgi cell network (De Zeeuw et al., 2008). In addition to these slow oscillations, local field oscillations have been found to occur at 30-80 Hz (gamma band), 80-160 Hz (high gamma band or very fast oscillations) and 160-260 Hz (low amplitude, very high frequency oscillations) (De Zeeuw et al., 2008).

In the primate cerebellum, LFPs recorded in the paramedian and simple lobules and Crus I and Crus II of the granule cell layer occur within a 10-25 Hz range and have been shown to be modulated by behavior (Pellerin & Lamarre, 1997). More precisely, they occur when the animal is immobile yet still attentive to its environment (Pellerin & Lamarre, 1997). Performance of an elbow flexion task results in modulation of the LFPs;

they are decreased before movement occurs, disappear during movement, and increase after movement (Pellerin & Lamarre, 1997). Figure 2 illustrates the modulation of LFP oscillations during the behavioral motor task. In further studies by Courtemanche, Pellerin and Lamarre (2002), these oscillations appeared to be related to the animals' state of expectancy: removal of the movement component, the elbow flexion task, (resulting in the "passive expectancy" state) resulted in stronger oscillations. In addition, oscillatory activity in the 7-8 Hz frequency range was observed to occur in the Crus IIa area of the granule cell layer of the cerebellum in unrestrained rats while they were immobile but attentive; movement of the animal resulted in cessation of the oscillations (Hartmann & Bower, 1998).

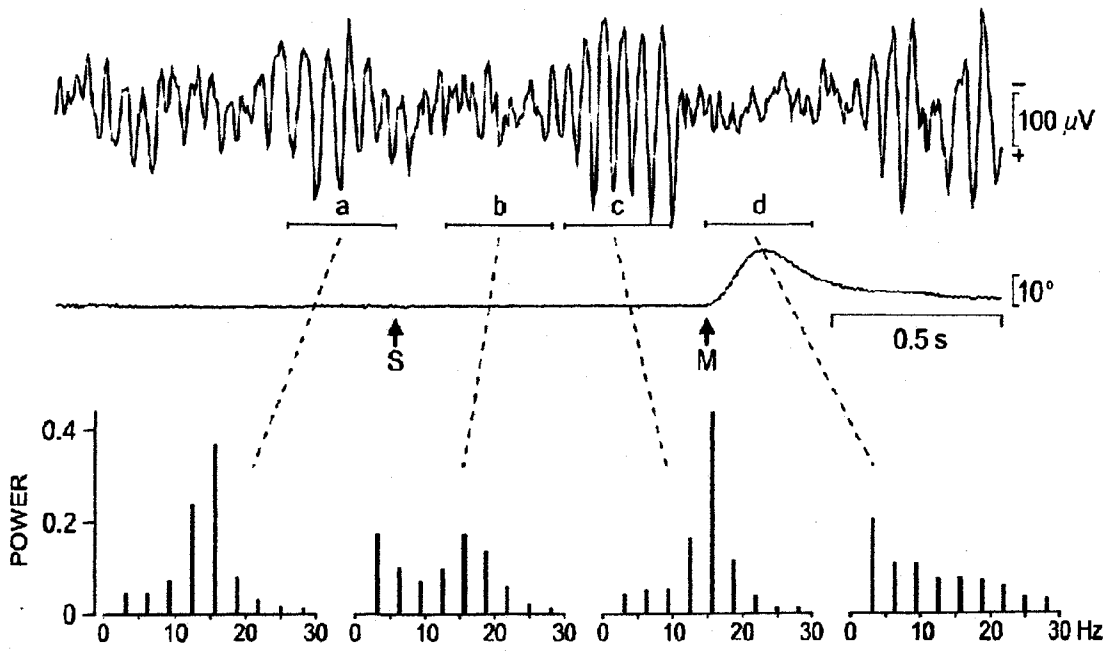

Figure 3

Behavioral Motor Task Modulates LFP Oscillations

Upper trace: LFPs during a 3s behavioral trial where the monkey performed a flexion of the arm (M) following the onset of an auditory cue (S). Middle trace: Movement trace. Bottom trace: Power spectra from 320 trials were calculated for 4 320ms windows (a-d). Adapted from Pellerin & Lamarre, 1997.

In simultaneous recordings from the paramedian lobule and the primary somatosensory cortex (S1) in primates, active stimulus expectancy synchronizes cerebellar and S1 LFPs (Courtemanche & Lamarre, 2005). This synchronization is thought to reflect network dynamics and communication between these areas that may promote effective somatosensory processing to perform a task (Courtemanche & Lamarre, 2005). Besides rhythmicity and synchronization of LFPs, phase coding of neural activity has also been investigated in the cerebellum. In the cerebellar cortex, parallel fibers have the ability to synchronize spontaneous activity in Golgi cells that may lead to the latter's ability to control the timing of granule cell spiking (Vos, Maex, Volny-Luraghi, & De Schutter, 1999). Also, simple spike discharges of Purkinje cells is phase related to the timing of cerebellar population activity as measured by LFPs (Chen, 2003). Courtemanche et al. (2002) found that simple spikes from Purkinje cells are phase locked with peaks of LFPs that may be related to the plausible effect of the granule cell layer oscillations on the cortex output (Courtemanche, Pellerin, & Lamarre, 2002). These findings suggest that cerebellar cortex oscillations may contain information that could influence other distinct brain areas, such as S1. Similar temporal relationships between single-unit activity and LFPs have also been shown to occur in neocortical and hippocampal recordings (Buzsaki, 2002; Gray & Singer, 1989).

Importance of Climbing Fiber Input

As mentioned previously, low frequency, 1 to 10 Hz, firing of climbing fibers in the inferior olivary nucleus is transmitted to the Purkinje cells in the cerebellar cortex

resulting in a complex spike (Devor, 2002). In addition, the spatial distribution and properties of a variety of ionic channels of olivary neurons give them the ability to generate rhythms (Devor, 2002) These subthreshold membrane oscillations range from 5-12 Hz and the output of the olivary neurons is phase locked to the depolorizing phase of the cycle (Devor, 2002). Inferior olive neurons are electrically coupled by gap junctions and are required for grouping of synchronous oscillatory activity but not for the generation of these rhythms (Leznik & Llinas, 2005). While present in a different layer, these network oscillations could possibly interact with the theta oscillations recorded from the granule cell layer of the cerebellar cortex, together forming a timing structure for cerebellar cortex output.

Neurochemical Circuits and LFPs

Regulation and integration of synaptic transmission within neuronal circuits is fundamental for information processing in the cerebellum (Nakanishi, 2005). The cerebellar cortical network's synaptic transmission is mediated through the excitatory action of glutamate and modulated by inhibitory GABA (Nakanishi, 2005). The highest density of specific receptors for GABA throughout the brain is found in the cerebellum on granule cells that are the most abundant cells in the cerebellum (Labrakakis, Muller, Schmidt, & Kettenmann, 1997; Mohler, 2006). $GABA_A$ receptor activation leads to an increase in permeability of the cell to Cl^- that is responsible for the inhibitory effect on granule cells (Labrakakis et al., 1997). $GABA_A$ receptors can be blocked by antagonists such as picrotoxin and bicuculline and activated by agonists like muscimol (Cooper, 2003; Labrakakis et al., 1997). Golgi cells receive excitatory input from parallel fibers

and consequently suppress granule cells through tonic and phasic mechanisms using GABA by activating $GABA_A$ receptors (Labrakakis et al., 1997; Nakanishi, 2005; Rossi, Hamann, & Attwell, 2003).

Synchronous oscillations in the granule layer of the cerebellum could be generated through the dynamics of the granule cell-Golgi cell circuit (De Schutter & Bjaalie, 2001). The connectivity of cerebellar Golgi and granule cells is depicted in Figure 4. Inhibition of granule cells can occur through feed forward or feedback pathways (Maex & De Schutter, 1998). In the feed forward pathway, mossy fibers excite Golgi cells which inhibit granule cells (Maex & De Schutter, 1998). In the feedback circuit, mossy fibers excite granule cells which inhibit parallel fiber excitation of Golgi cells that would normally inhibit granule cells (Maex & De Schutter, 1998).

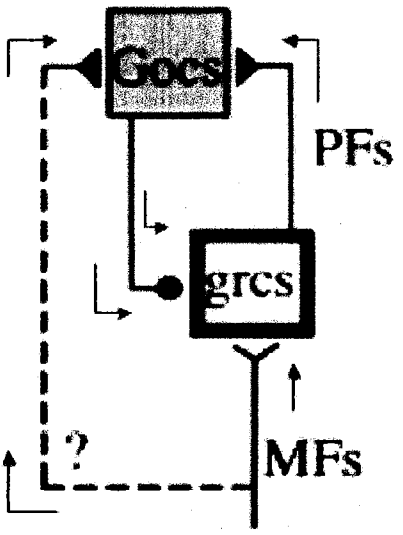

Figure 4

Pathways for Inhibition to Granule Cells

Red arrows indicate the feedback pathway and blue arrows depict the feed forward pathway. Gocs: Golgi cells, grcs: granule cells, MFs: Mossy fibers, PFs: Parallel fibers. Adapted from Maex & De Schutter, 1998.

The circuit is allowed to oscillate due to parallel fiber excitation that couples the Golgi cells in a synchronous rhythm and the feedback inhibition to granule cells which couples the granule cell rhythm to that of the Golgi cells (Maex & De Schutter, 1998). The rhythmicity in the cerebellar LFPs could result from afferent input from mossy fibers or may be generated by the granule-Golgi cell circuit (Courtemanche et al., 2002). In addition, synchronous oscillations in the granular layer would result in transmitting regular parallel fiber spikes to Purkinje cells along with filtering of input from mossy fibers (Maex & De Schutter, 2005). The only definitive test to determine if these LFPs are generated by the granule-Golgi cell circuit would be to cut peripheral afferents coming into the cerebellum and still have rhythmic oscillations, however, Golgi and granule cells are increasingly believed to be intrinsic oscillators (Maex & De Schutter, 2005).

Cerebellar Oscillatory Activity In Vitro

In addition to oscillations recorded in vivo, some in vitro studies have also shown interesting results with respect to granule cell layer synaptic connections and rhythmic activity. Some neurons have a favored input frequency that promotes an enhanced oscillatory response, a property called resonance (D'Angelo et al., 2001). Cerebellar granule cells have been shown to resonate at theta frequencies due to a slow K^+ current (D'Angelo et al., 2001). A mathematical model of granule cell excitability proposed by Dangelo et al (2001) showed that I_{NA-P} and I_{K-SLOW} were sufficient to generate regular theta- frequency oscillations that were then eliminated when either current was turned off. In addition, several ionic mechanisms have been implicated in the pacemaking

properties of Golgi cells in vitro; a potent hyperpolorization-activated current (I_h) and subthreshold Na^+ currents ($I_{Na+,sub}$) are enough to sustain feed-forward depolarization and delayed repolorizing feedback involves an M-type K^+ (I_M) like current (Forti, Cesana, Mapelli, & D'Angelo, 2006). Lastly, this Golgi cell pacemaking property could affect the cyclic inhibition exerted by Golgi cells onto the cerebellar granule cell layer by offering a means for fine adjustments of firing frequency and precision (Forti et al., 2006). In addition, the network oscillations observed in the cerebellar granule cell layer of rats and primates (Hartmann & Bower, 1998; Pellerin & Lamarre, 1997) could be explained by this cyclic inhibition.

Rationale

Functional brain mapping reveals aspects of the localization of natural phenomena to examine the organization within a particular brain region (Toga, 2002). Electrophysiological mapping methods have focused primarily on mapping motor output in response to electrical stimulation (Toga, 2002). The mapping of brain oscillations through the use of recorded LFPs is a valid means to characterize network activity based on the anatomical structures and pathways of different areas in the cerebellum. In addition, localization of higher oscillating areas in the cerebellum could give insight to the dynamics and functional circuits that cause this phenomenon.

Objectives and Hypothesis

In this experiment, electrophysiological recordings have been used to determine the functional topography and spatial characteristics of granule cell layer oscillations in

the cerebellum. Given that the more posterior vermal and hemispheric lobules receive an abundant amount of afferent input and a strong input from cerebral cortex areas that themselves can show oscillations, stronger 5-10 Hz oscillation areas could occur at specific locations in the cerebellar cortex granule cell layer.

Methods

Subjects and Behavior

Four male Sprague-Dawley rats were used in this research experiment. Initially, the rats were handled and manipulated daily as to get familiarized with the laboratory environment and researchers. All the rats weighed between 250 and 300g upon arrival to the animal care facility and were housed in pairs in plastic cages with no restrictions to food or water on a 12-hour light/dark cycle. Rats were habituated to their environment over a few weeks: rats were placed in a Lafayette Instruments ABET System (Lafayette, IN, USA) operant conditioning box. However, rats were not engaged in a task when placed in this conditioning box and recordings from subjects were made during a resting behavioral state characterized by immobility.

Surgery and Implantation

Prior to surgery each rat, now weighing between 400 and 600 g, was anesthetized with injections of ketamine (100 mg/kg), xylazine (8mg/kg) and atropine (0.4 mg/kg) with booster doses available when needed. Body temperature was controlled through the use of a heating pad and measured by means of a rectal thermometer. Each rat was placed in a stereotaxic apparatus with the dorsal surface of the skull exposed after shaving and cleaning of the head. Implantation of a head stage, usually aimed at 12mm posterior to bregma and 3mm lateral of midline, in the cerebellar cortex of each rat permitted the recording of LFPs and single unit activity simultaneously. The implantable head stage consisted of 2 to 8 single fine epoxylite-covered tungsten microelectrodes (0.5-4 MΩ) on freely movable microdrives that entered in a 19G needle tip casing. Needle tip casings

were used as a protective shield for microelectrodes at the time of dura penetration during implantation. Each needle could house a maximum of 2 single microelectrodes. Figure 5 illustrates the implantation site and head stage. During surgery, 6 screws were screwed into the skull and covered with dental acrylic cement to form a stable base. Each rat was administered buprenex (0.02 mg/kg) post-surgery and a recovery time of three days was provided before commencement of neurophysiological recordings.

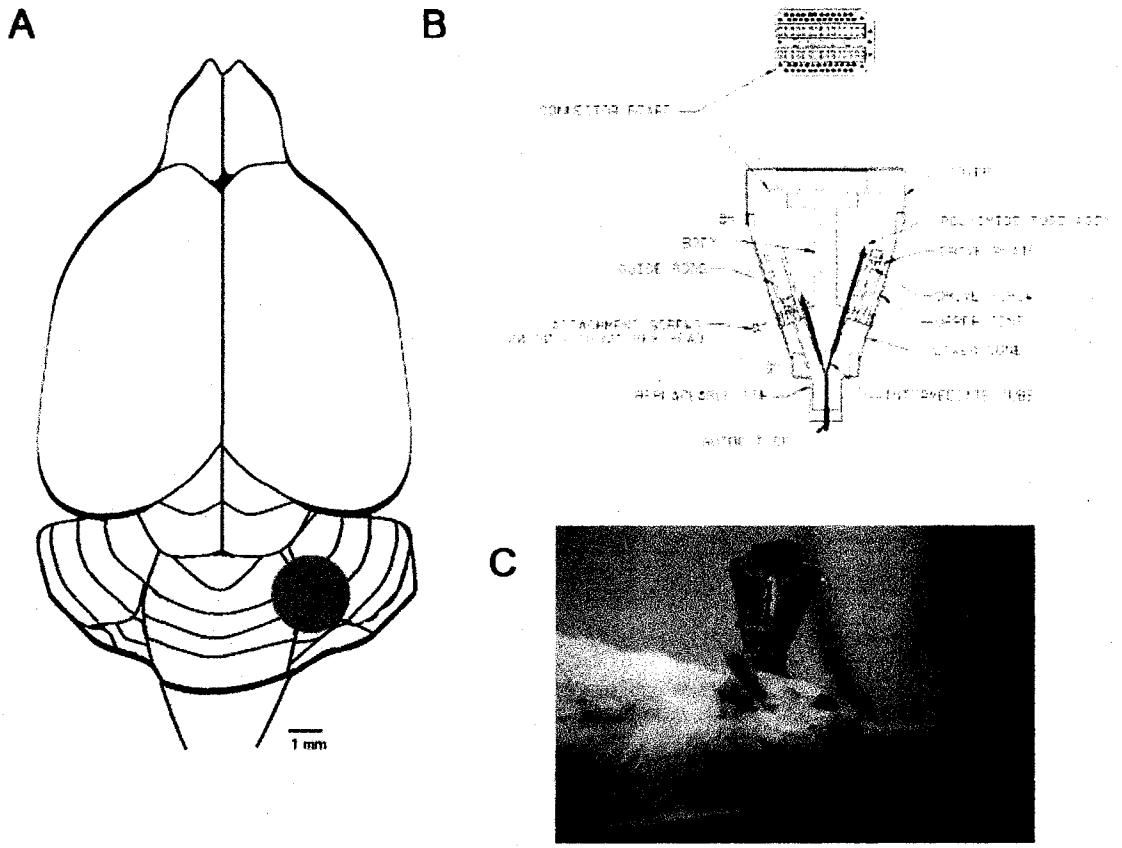

Figure 5

Implantable Head Stage

A. Schematic drawing of the dorsal view of a rat brain, projected implantation site is represented by the purple shaded area. B. Internal body of microdrive assembly and connector board. During neurophysiologic recordings, a preamplifier is connected to a pin connector held at the top of the inner body. The plastic cone and removable cover protect the microdrives. Each microelectrode is held inside tubings that are connected to a mobile piece. By turning a drive screw, the top piece moves along a supporting rod and the microelectrode enters into a guide tube that then comes out and can be lowered or raised in the brain tissue (adapted from Jog et al., 2002). C. The head stage was fitted with between 2 and 8 independently moveable fine epoxylite-covered tungsten microelectrodes (0.5 – 4 MΩ).

Neurophysiological Recordings

Neurophysiological recordings lasted a few weeks in each rat. Unipolar recordings were made at regular 0.25 to 0.5 mm intervals, or upon a change in layers, especially the granule cell layer, or when capturing a single unit. In addition, this method was able to differentiate between Purkinje cells (presence/absence of complex and simple spikes) and interneurons such as Golgi cells, basket cells, and nuclear activity. Unit activity was monitored but it will not be reported here. Multi-unit activity was used as a guide to monitor track advancement. All data was acquired through the use of the Neuralynx Cheetah system (Tuscon, AZ, USA) that allowed up to 24 channels of single unit recording and 8 LFP channels. LFP and action potential signals from each channel were filtered at 1-125 Hz and 600-6000 Hz bandwidth respectively. The digitization rate was 2003 Hz. The head stage ground was attached to one of the screws in the skull whereas the reference was situated in one of the needle tip casings that ended in the cerebellar tissue.

Histological procedures

On completion of the last recording session, electrolytic lesions were made using anodal current pulses between 200-300 μA and lasting 1.5-2.5 mins generated with a Grass S88 Stimulator equipped with a current control unit and a stimulus isolation unit. The animals were then perfused and the brain was immersed in formaline, followed after a few days in 30% sucrose formaline. The cerebellum was sliced sagittally in a cryostat at 30 to 50 μm thick sections and stained using cresyl violet. Histological procedures allowed confirmation of electrode placements in the cerebellar slices.

Data Analysis

All analyses were made using NeuroExplorer (Nex technologies, Littleton MA), MS Excel and Statistica software. LFPs were analyzed using Fast Fourier Transforms (FFTs) to evaluate rhythmicity. All LFPs analyzed were initially visually inspected to remove any stretches containing saturations and noise (often artifacts from movement of subjects); hence we considered the remaining time periods as valid recording periods. In addition, for an LFP recording to be considered valid it was a minimum of 5 seconds long. Rhythmicity in the 5-10 Hz range was quantified by calculating the proportion of the power spectral densities in the FFT spectrum within these boundaries for consecutive time windows of 500 ms throughout valid recording periods. This analysis identified time windows with a higher oscillatory proportion of the signal. Figure 6 depicts the flow of data analysis from raw data to a value of oscillatory %.

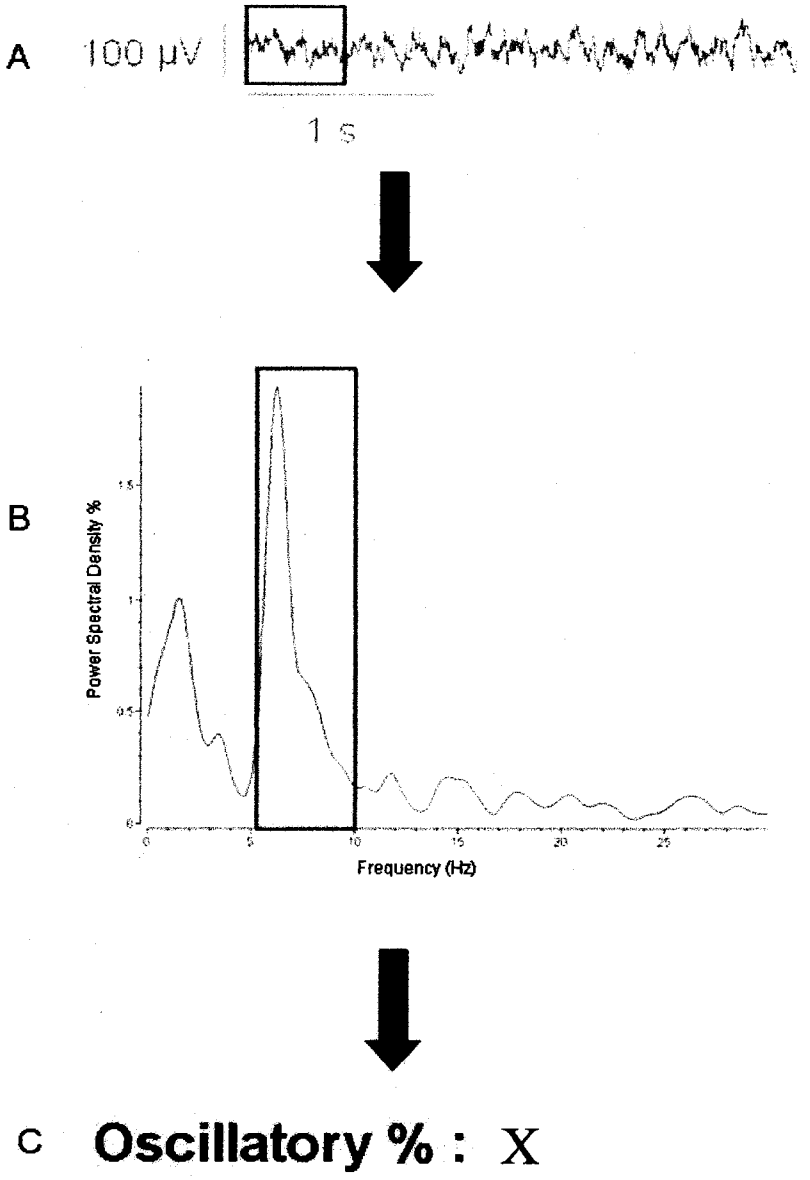

Figure 6

Data Analysis

A. A sliding time window of 500ms throughout valid recording periods. B. Spectrogram is generated to determine the Oscillatory %, the area under the power spectral density curve in the 5-10 Hz range for each window C. This value corresponds to a data point at each depth, each depth has a minimum of 100 data points.

In order to spatially differentiate areas of increased rhythmic activity and create a three-dimensional map of oscillations in the cerebellar granule cell layer, categorical variables "region" and "position" were created. In each rat, recording sites were categorized by their relative depth, in three subdivisions. Each defined region represents 1/3 of the overall depth of the longest recording track, with subdivision 1 being most superficial and subdivision 3 deepest. For each cerebellar region, the mean of the areas under the power spectral density (PSD) curves for corresponding depths were calculated. For relative position, we aimed at three targets within the implantation site when considering the cerebellum in the transverse plane: (1) lateral caudal, (2) lateral rostral, and (3) medial rostral. Figure 7 depicts the 3 regions of the cerebellum and the arrangement of aimed position targets.

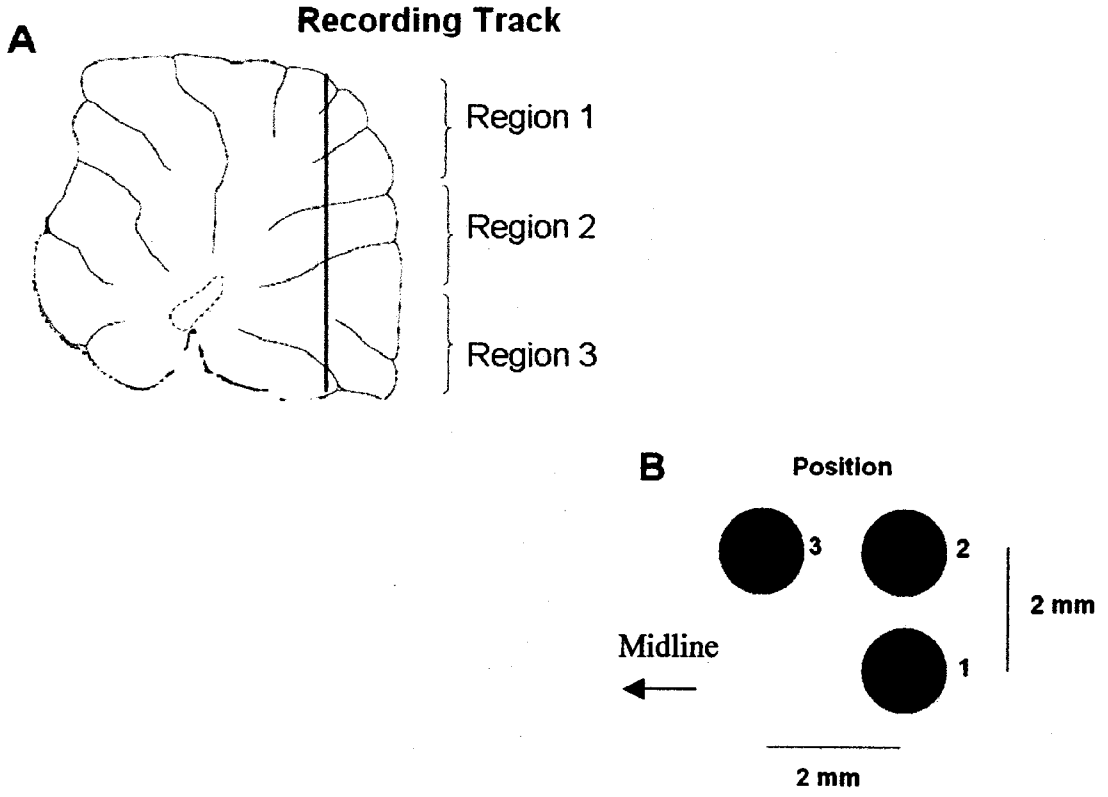

Figure 7

Regions and Positions

A. Recording sites were categorized by their relative depth, in three subdivisions. Each defined region represents 1/3 of the overall depth of the longest recording track, with subdivision 1 being most superficial and subdivision 3 deepest. B. Three targets within the implantation site for mapping the cerebellum in the transverse plane: (1) lateral caudal, (2) lateral rostral, and (3) medial rostral.

Following the analysis of the relationship between position and region with rhythmic activity, data was processed to identify which lobules of the cerebellum have increased oscillatory activity. Initially, lesions were identified and associated to a particular lobule. The subsequent associations of particular regions and positions to cerebellar lobules without lesions were made by means of a rat atlas (Paxinos, 1998) and computations involving turns and electrode depth. Finally, once each rat had an identified lobule that corresponded to a particular Region and Position, a one-way ANOVA was used to determine which lobule showed increased rhythmic activity. After histological confirmation of the lobules associated to each lesion and knowing which region and position they occur in, the remaining regions at each position in both rats were associated to a lobule. To properly classify each region at each position as an associated lobule, the rat atlas and computations on recording track limits (1 turn = 0.16 mm) were used. As mentioned previously, each defined region represents 1/3 of the overall depth of the longest recording track, therefore the amount of turns that constitute the interval of recording track limits and the recording track length for each region is standard for each rat. The associated lobule was identified by using the length of the recording track calculated from the interval of the track limit and sagittal images from a rat atlas at different ML-AP coordinates.

Statistics

A t-test for independent samples was performed to determine if the oscillatory activity of adjacent microelectrodes in the same needle were similar. Z-scores for both needles were used to compare the observations from different normal distributions.

Correlations were used to examine the relationship between oscillatory activity and microelectrode depth. This permitted to identify trends considering the independent variable for mapping we had the most control over, so the depth of the microelectrode going through the cerebellar cortex layers. In addition, the variations on oscillatory activity according to anterior-posterior (AP) and medial-lateral (ML) location was examined by means of one-way ANOVAs with the plane as a factor. As there is a possible interaction between our variables i.e. the different planes (depth, AP, and ML), we proceeded in the analysis of this interaction by assigning a factorial element to depth (region) and position. To determine the interaction of region and position on oscillatory activity a multi factorial ANOVA (MANOVA) was used. Tukey HSD post hoc tests were used to assess which comparisons were significant after obtaining a significant difference in ANOVAs. The level of significance was set to $p < 0.01$.

Results

The following section will present the results of mapping local field potential oscillations in the rat cerebellar cortex granule cell layer.

Firstly, the general features of subjects will be presented. The documented weights, precise implantation site coordinates, number of recording sessions, recording sites and time windows are documented below and in Table 1. Following the identification of subject characteristics, the presence of oscillations in the 5-10 Hz range during LFP recordings is shown. The oscillatory activity profile of microelectrodes in the same and different needles is then presented. In particular, the comparisons of recordings from electrodes in the same needle and at the same depth, same needle and at different depths and different needles at the same depth are shown. As a primary analysis of the mapping of LFPs in the rat cerebellar cortex granule cell layer, the effect of electrode depth and location on oscillatory activity is demonstrated. The relationship between depth in the recording track, anteroposterior and mediolateral location with oscillatory activity is presented. The results of a secondary analysis on the relationship of oscillatory activity and the region-position interaction are then presented. In addition, the main effect of region and position on oscillatory activity is shown. Finally, the processing of data to identify which lobules of the cerebellum have increased oscillatory activity is demonstrated.

General Features of Subjects

For all rats, their weight at surgery, implantation site coordinates, number of recording sessions, number of recording sites and time windows was documented as presented in table 1. The weight of all four rats is between 370g and 570g at surgery. The center of the recording head stage was implanted at the implantation site coordinates listed for each rat. The small difference in coordinates of implantation sites between rats occurs due to the measurement adjustments made during surgery because of the size of the rat. Recording sessions are the amount of times that each rat was recorded from. It is important to note that during each recording session it was possible to record from different sites. In addition, the recording sessions were made over a period of 1-2 months in all rats. The number of recording sites for individual microelectrodes represents the number of distinct depths where recordings were made. Time windows are the total number of 500 ms time windows analyzed from valid recording periods.

Rat	Weight at Surgery (g)	Implantation Site Coordinates (mm)	Recording Sessions	Recording Sites	Time Windows
1	470	Anterior-Posterior : -12.5 Medial-Lateral: -3.0	18	Electrode 1: 9 Electrode 2: 3 Electrode 3 : 10 Electrode 6: 7 Electrode 7: 2	1327 1327 1327 1327 1327
2	370	Anterior-Posterior : -12.5 Medial-Lateral: -3.0	12	Electrode 1: 6 Electrode 2: 5 Electrode 4: 4 Electrode 5: 5 Electrode 6: 1 Electrode 7: 1 Electrode 8: 3	999 999 900 790 790 680 680
3	545	Anterior-Posterior : -12.5 Medial-Lateral: -2.5	10	Electrode 1: 6 Electrode 2:11 Electrode 3: 13 Electrode 4: 8	1978 2342 2342 2342
4	570	Anterior-Posterior : -13.5 Medial-Lateral: -3.0	13	Electrode 3 : 10	2573

Table 1

General Features of Subjects and Measurements

From left to right columns indicate: (1) Rat identification; (2) Rat weight at surgery in grams; (3) Precise coordinates of center of implantation site; (4) Number of recording sessions in days; (5) Number of recording sites for individual electrodes; (6) Total number of 500ms time windows.

Presence of Oscillations in 5-10 Hz range During LFP Recordings

Oscillations in the 5-10 Hz range were present in neurophysiological recordings. The presence of oscillations in the 5-10 Hz range was assessed by calculating the PSD, via the Fast Fourier Transforms for recording periods of 500 ms intervals. As demonstrated by Figure 8, LFP recordings that contained less activity in the 5-10 Hz range had lower frequency variations or desynchronized activity. Recordings that were oscillatory showed a shift in the peak of PSD % to frequencies in the 5-10 Hz range.

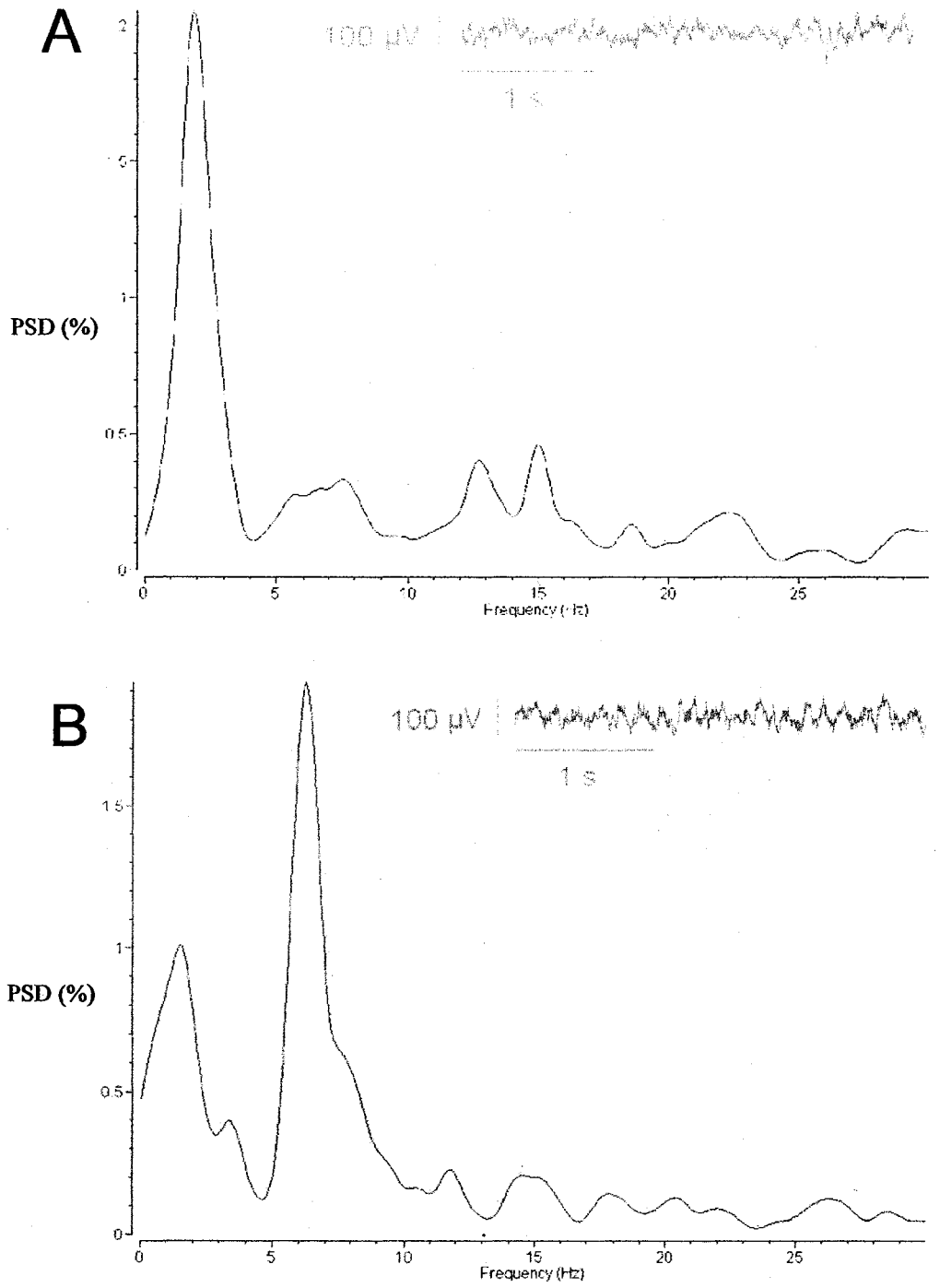

Figure 8

Examples of LFP Recordings and Corresponding FFT from the Same Electrode.

A. LFP recording of non-oscillatory activity with the corresponding FFT showing low PSD % values in the 5-10 Hz range. B. LFP recording of oscillatory activity peaking at 7 Hz with the corresponding FFT.

Oscillatory Activity Profile of Microelectrodes in the Same and Different Needles

LFP signals average voltage across a small amount of neural tissue, therefore, microelectrodes in a close vicinity should record similar field potentials. To determine if the oscillatory activity of adjacent microelectrodes in the same needle were similar, a t-test for independent samples was performed. Z-scores for both needles were used to compare the observations from different normal distributions. The box and whisker plot in Figure 9 demonstrates that microelectrodes in the same needle are not significantly different from each other throughout recordings at $p = 0.135$. In addition, regression scatterplots were performed to describe the degree of the relationship with oscillatory activity between two microelectrodes at the same depth in the same needle, two microelectrodes at different depths in the same needle and two microelectrodes at the same depth in different needles. Figure 10 shows the correlations for the conditions mentioned previously. Electrodes 2 and 7 at a depth of 18 turns and in the same needle showed a strong correlation value of $r = 0.788$ at $p < 0.001$. Electrodes 2 and 7 at a depth of 28 and 18 turns respectively and in the same needle showed a weaker correlation value of $r = 0.394$ at $p < 0.001$. Lastly, electrodes 6 and 7 at a depth of 18 turns and from different needles showed the weakest correlation value of $r = 0.238$ at $p < 0.001$. Briefly, microelectrodes in the same needle and at the same depth record similar field potentials whereas there is a loss of similarity of recordings when they are from different depths and needles.

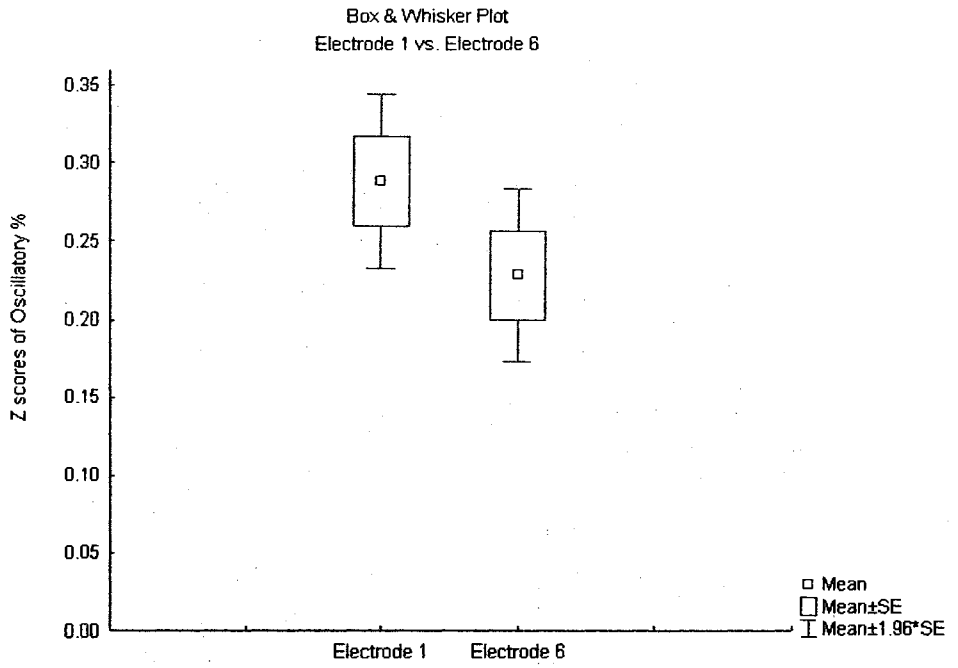

	T-test for Independent Samples Note: Variables were treated as independent samples										
Group 1 vs. Group 2	Mean Group 1	Mean Group 2	t-value	df	p	Valid N Group 1	Valid N Group 2	Std.Dev. Group 1	Std.Dev. Group 2	F-ratio Variances	p Variances
Electrode 1 vs. Electrode 6	0.287935	0.228006	1.495760	2652	0.134835	1327	1327	1.036188	1.027890	1.016211	0.769732

Figure 9

Oscillatory Activity Profile of Microelectrodes in the Same Needle

Mean and standard deviation of the z-score for the percentage of oscillatory activity between microelectrodes situated in the same needle irrespective of depth. Microelectrodes in the same needle are not significantly different from each other throughout recordings as demonstrated by a t-test for independent samples. $p = 0.135$.

Same Needle, Same Depth

A

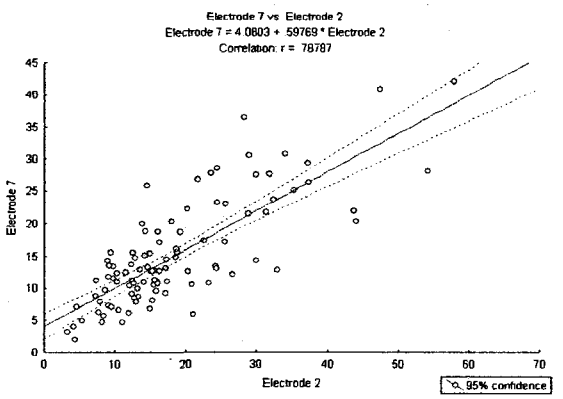

Same Needle, Different Depths

B

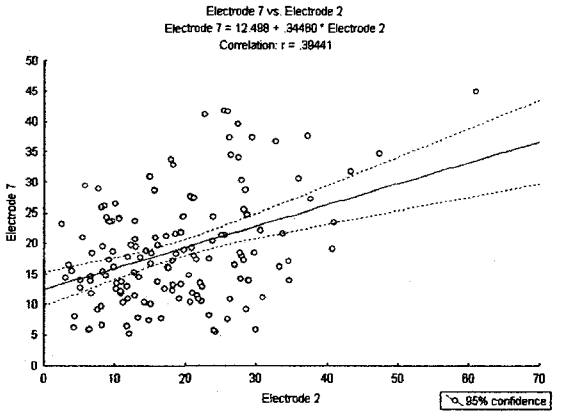

Different Needles, Same Depth

C

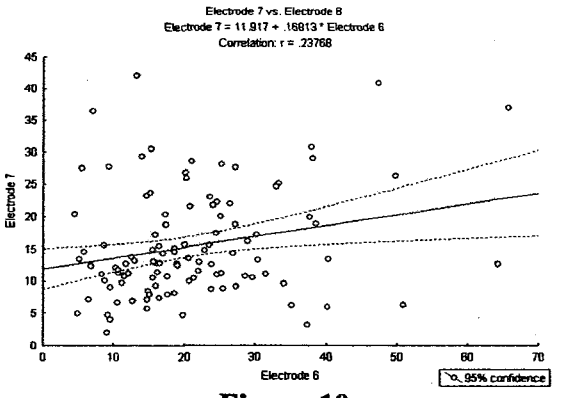

Figure 10

Oscillatory Activity Profile of Microelectrodes in the Same and Different Needles

A. Electrodes 2 and 7 at a depth of 18 turns and in the same needle showed a strong correlation value of $r = 0.788$ at $p < 0.001$. B. Electrodes 2 and 7 at a depth of 28 and 18 turns respectively and in the same needle showed a weaker correlation value of $r = 0.394$ at $p < 0.001$. C. Electrodes 6 and 7 at a depth of 18 turns and from different needles showed the weakest correlation value of $r = 0.238$ at $p < 0.001$.

Effect of Electrode Depth on Oscillatory Activity

One of the controlled variables in this experiment is electrode depth. As a first analysis, multiple regression scatterplots were performed for each of the 4 rats to determine the relationship between electrode depth and oscillatory activity. In addition, the pooled data of all 4 rats was examined by the same method. Figure 11 shows that oscillatory activity was positively correlated with depth for rats 1, 2 and 4 ($r = 0.252$, $p < 0.001$ for rat 1, $r = 0.097$, $p < 0.001$ for rat 2 and $r = 0.253$, $p < 0.001$ for rat 4). Rat 3 showed a negative correlation between oscillatory activity and depth ($r = -0.051$, $p < 0.001$). When all of the data was pooled together, oscillatory activity was positively correlated with depth ($r = 0.066$, $p < 0.001$). It is important to note that in each rat and at all depths there is a notable spread of data points in relation to oscillatory %. This occurs because each individual data point represents the oscillatory activity within 5-10 Hz of the PSD for multiple time windows during recordings. Since oscillations do not occur during the whole length of recordings and they are only a transient phenomenon, there is a varied spread of oscillatory % at each depth.

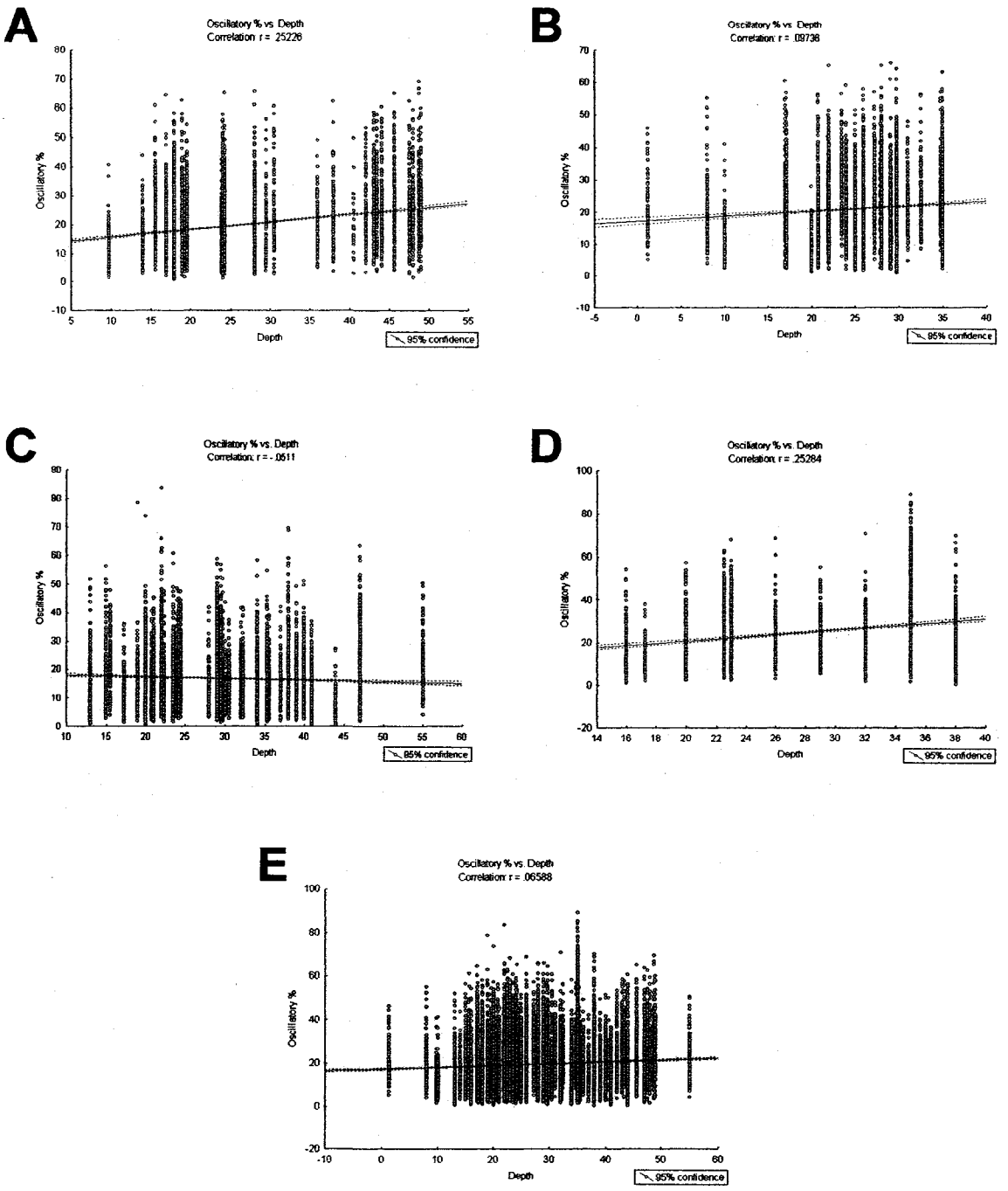

Figure 11

Effect of Electrode Depth on Oscillatory Activity in the Cerebellum

Oscillatory activity was positively correlated with depth for rats 1, 2 and 4 and negatively correlated for rat 3. A. $r = 0.252$, $p < 0.001$ for rat 1. B. $r = 0.097$, $p < 0.001$ for rat 2. C. $r = -0.051$, $p < 0.001$. D. $r = 0.253$, $p < 0.001$ for rat 4. E. Oscillatory activity was positively correlated with depth ($r = 0.066$, $p < 0.001$) for pooled data.

Electrode Location on Oscillatory Activity

Anterior-posterior and medial-lateral steriotaxic planes were also controlled variables in this experiment. As a first analysis in the transverse plane, a one-way ANOVA was calculated. Results of the one-way ANOVA in the anterior-posterior (AP) plane revealed significant differences in oscillatory % at different locations; $F(2, 24047) = 468.5$, $p < 0.01$. Most strikingly, increased oscillatory activity occurred at -12.5 mm and -13.5 mm whereas rhythmic activity at -11.5 mm was less. A Tukey HSD post hoc test showed that all groups were significantly different from each other. Figure 12 depicts both the one-way ANOVA and Tukey HSD comparisons for AP location and oscillatory %. In addition, one-way ANOVA also revealed significant differences in oscillatory % at different locations in the medial-lateral (ML) plane; $F(2, 24045) = 78.75$, $p < 0.01$. The most rhythmic activity occurred at location 3.5 mm, followed by 2 mm, 4 mm, 1.5 mm and 3 mm from the midline. The Tukey HSD post hoc test depicts that several pairs of groups were significantly different. Figure 13 depicts both the one-way ANOVA and Tukey HSD comparisons for ML location and oscillatory %. In short, significant differences in oscillatory activity were observed to occur at different AP and ML coordinates in the transverse plane.

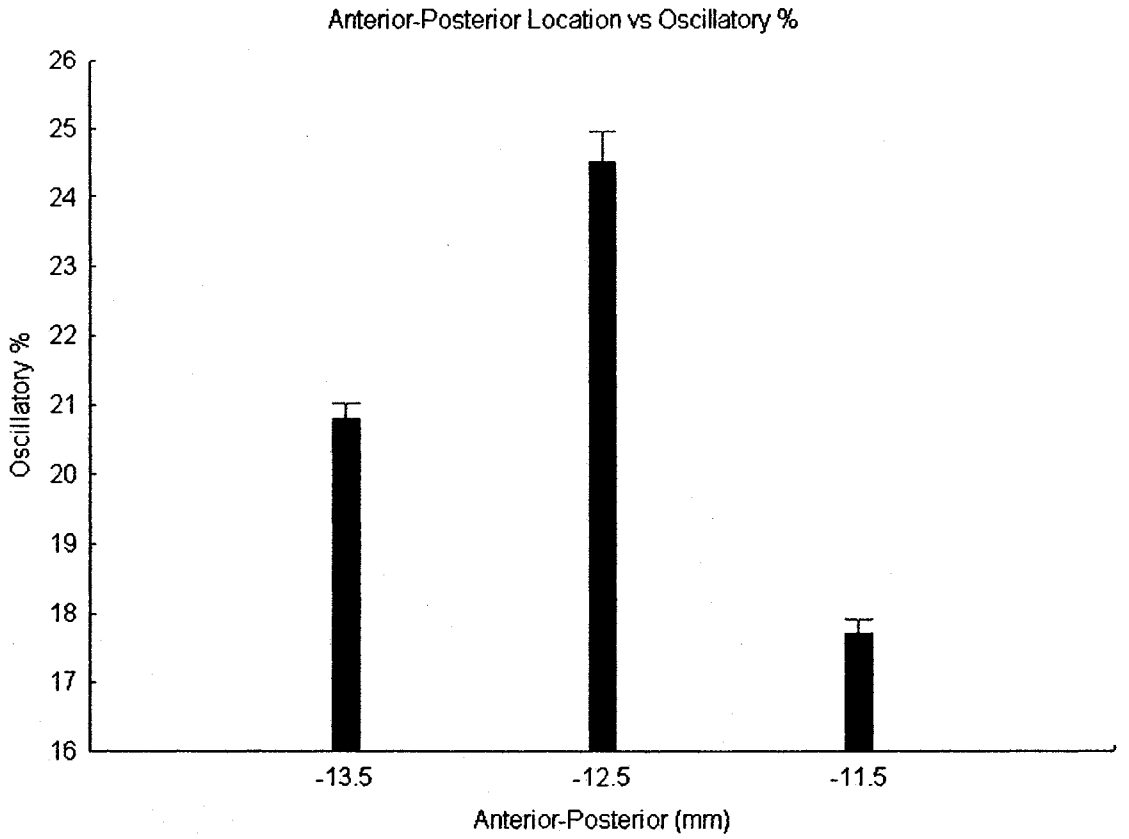

Cell No.	Anterior-Posterior	{1} 20.789	{2} 24.519	{3} 17.696
		Tukey HSD test; variable Oscillatory % Approximate Probabilities for Post Hoc Tests Error: Between MS = 128.23, df = 24047.		
1	-14		0.000022	0.000022
2	-13	0.000022		0.000022
3	-12	0.000022	0.000022	

Figure 12

Anteroposterior Location in the Transverse Plane and Oscillatory Activity in the Cerebellum

One-way ANOVA of oscillatory % at different anterior-posterior locations and Tukey HSD post hoc comparisons. All groups are significantly different from each other. $F(2, 24047) = 468.5$, $p < 0.01$.

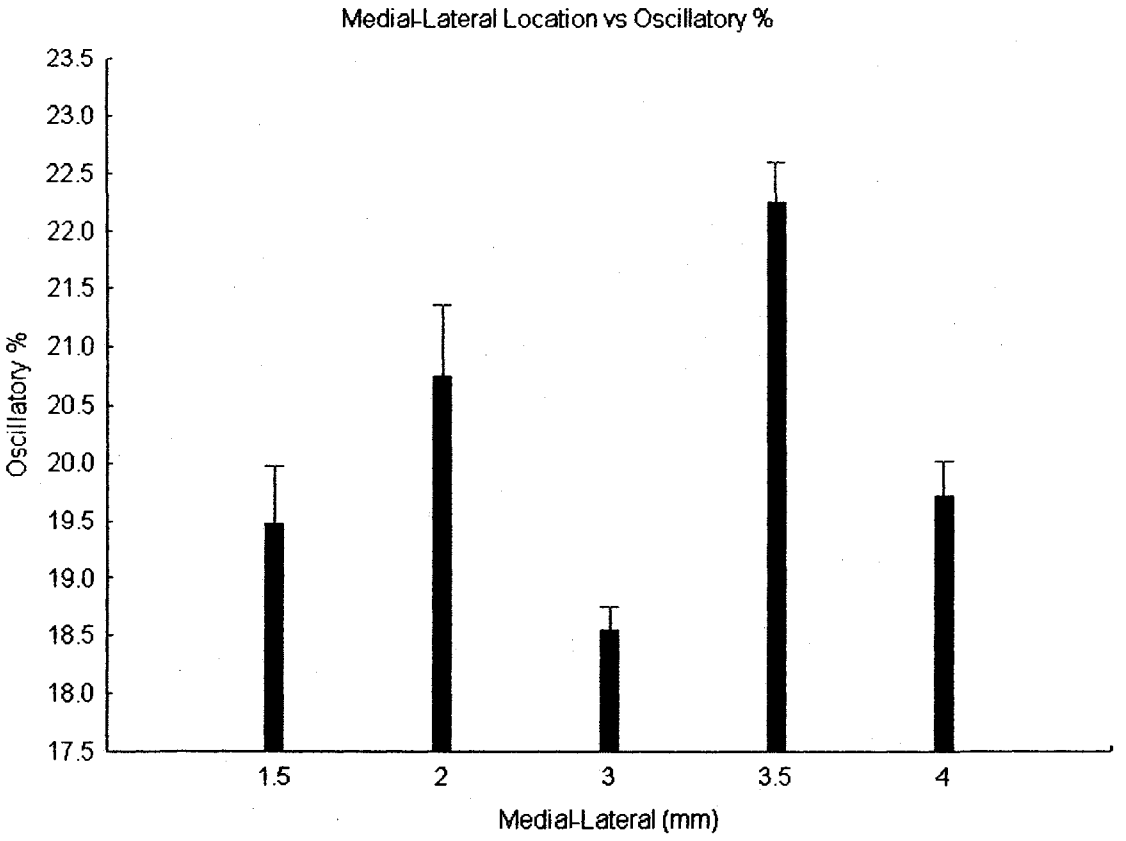

Cell No.	Medial-Lateral	{1} 19.465	{2} 20.744	{3} 18.542	{4} 22.234	{5} 19.708
	Tukey HSD test; variable Oscillatory % Approximate Probabilities for Post Hoc Tests Error: Between MS = 131.52, df = 24045.					
1	1		0.014148	0.008009	0.000017	0.928234
2	2	0.014148		0.000017	0.000446	0.026940
3	3	0.008009	0.000017		0.000017	0.000017
4	4	0.000017	0.000446	0.000017		0.000017
5	5	0.928234	0.026940	0.000017	0.000017	

Figure 13

Mediolateral Location in the Transverse Plane and Oscillatory Activity in the Cerebellum
One-way ANOVA of oscillatory % at different medial-lateral locations and Tukey HSD post hoc comparisons. Several pairs of groups were significantly different as depicted by the highlighted values in the post hoc table. $F(2, 24045) = 78.75$, $p < 0.01$.

Factorial Analysis: Oscillatory Activity and Region

The main effect of Region on oscillatory activity from the factorial ANOVA with Region and Position as factors revealed significant differences in oscillatory % at different regions in the cerebellum; $F(2, 24047) = 252.7$, $p < 0.01$. Most notably, oscillatory activity was lowest at Region 1 and highest at Region 3. The Tukey HSD post hoc test shows that all regions were significantly different from each other. Figure 14 depicts both the main effect and Tukey HSD comparisons for cerebellar region and oscillatory %.

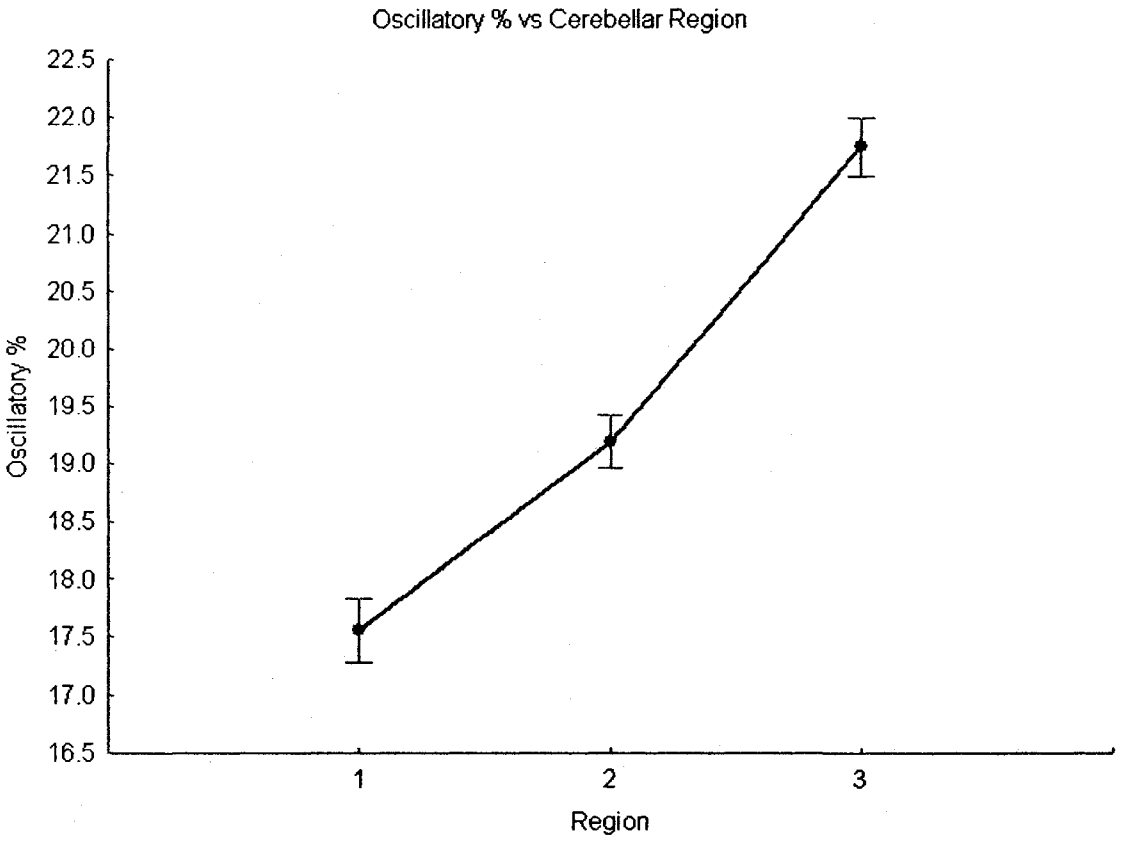

Cell No.	Region	{1} 17.563	{2} 19.186	{3} 21.737
1	1		0.000022	0.000022
2	2	0.000022		0.000022
3	3	0.000022	0.000022	

Tukey HSD test; variable Oscillatory %
Approximate Probabilities for Post Hoc Tests
Error: Between MS = 130.49, df = 24047.

Figure 14

Oscillatory Activity and Cerebellar Region

Oscillatory % at different cerebellar regions and Tukey HSD post hoc comparisons representing main effect from factorial ANOVA with region and position as factors. All groups are significantly different from each other. $F(2, 24047) = 252.7$, $p < 0.01$.

Factorial Analysis: Oscillatory Activity and Position

The main effect of Position on oscillatory activity from the factorial ANOVA with Region and Position as factors revealed significant differences in oscillatory % at different positions in the cerebellum; $F(2, 24047) = 449.8 p < 0.01$. Oscillatory activity was highest at Position 1 and lowest at Position 2. The Tukey HSD post hoc test shows that all positions were significantly different from each other. Figure 15 depicts both the main effect and Tukey HSD comparisons for position and oscillatory %.

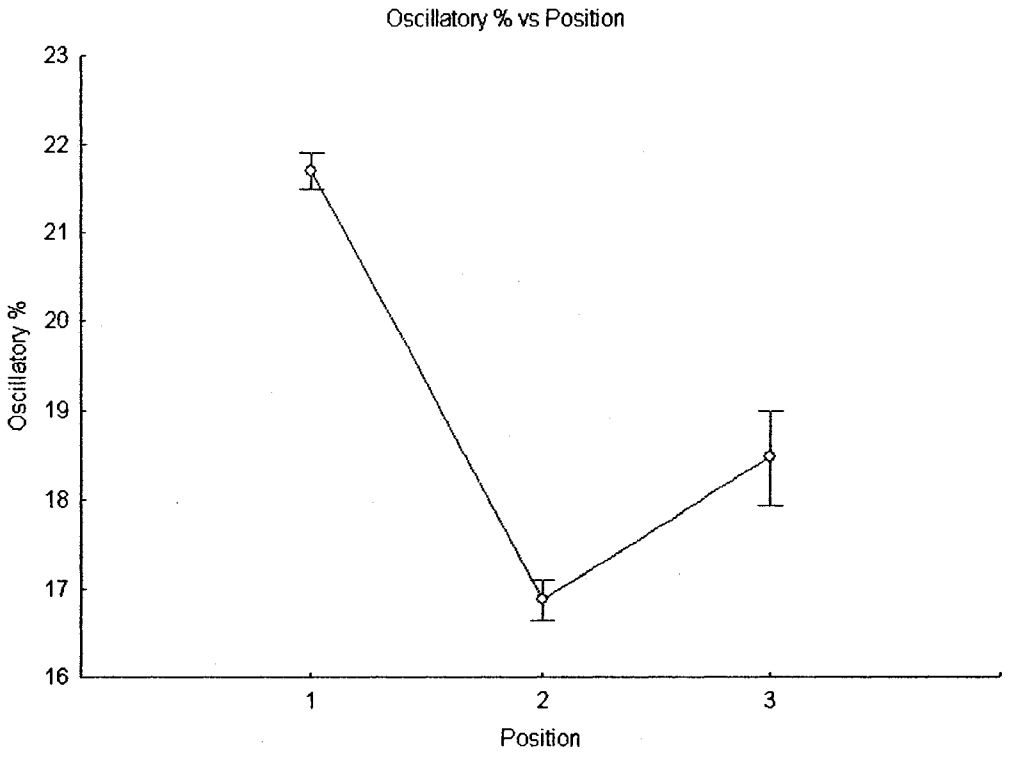

Cell No.	Position	{1} 21.616	{2} 16.866	{3} 19.947
		Tukey HSD test; variable Oscillatory % Approximate Probabilities for Post Hoc Tests Error: Between MS = 128.43, df = 24047.		
1	1		0.000022	0.000022
2	2	0.000022		0.000022
3	3	0.000022	0.000022	

Figure 15

Oscillatory Activity and Cerebellar Position

Oscillatory % at different cerebellar positions and Tukey HSD post hoc comparisons representing main effect from factorial ANOVA with region and position as factors. All groups are significantly different from each other. $F(2, 24047) = 449.8 p < 0.01$.

Factorial Analysis of Oscillatory Activity and Region-Position Interaction

A factorial ANOVA was used to test the interaction between Region and Position on oscillatory activity. A significant interaction was present for Region and Position on oscillatory activity $F(4, 24041) = 72.677$, $p < 0.01$. Analysis showed that at Position 1 there was a significant difference between the three regions, Region 3 showing the most elevated values of oscillatory activity ($F = 311.068$, $p < 0.01$). At Position 2 oscillatory activity was similar. Finally, for Position 3, only the oscillatory activity of Region 3 was significantly higher ($F = 46.073$, $p < 0.01$), while oscillatory activity at Position 1 and 2 were similar. The Tukey HSD post hoc test depicts that several pairs of groups were significantly different from each other. Figure 16 summarizes both the factorial ANOVA and the Tukey HSD post hoc test.

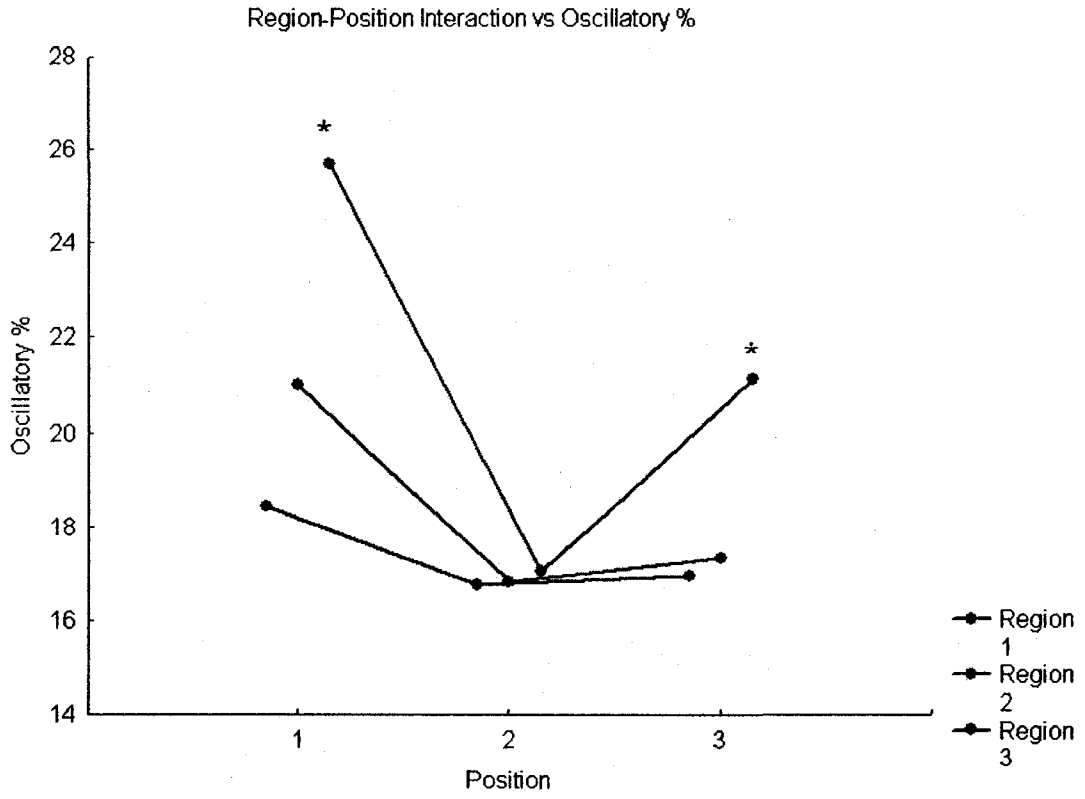

Cell No.	Region	Position	{1} 18.430	{2} 16.772	{3} 16.948	{4} 20.998	{5} 16.826	{6} 17.327	{7} 25.688	{8} 17.044	{9} 21.117
	Tukey HSD test; variable Oscillatory % (Sheet1 in NEW.stw) Approximate Probabilities for Post Hoc Tests Error: Between MS = 124.35, df = 24041.										
1	1	1		0.000011	0.044029	0.000010	0.000010	0.807977	0.000010	0.000192	0.000010
2	1	2	0.000011		0.999990	0.000010	1.000000	0.996889	0.000010	0.993905	0.000010
3	1	3	0.044029	0.999990		0.000010	0.999999	0.999927	0.000010	1.000000	0.000010
4	2	1	0.000010	0.000010	0.000010		0.000010	0.000012	0.000010	0.000010	0.999969
5	2	2	0.000010	1.000000	0.999999	0.000010		0.998366	0.000010	0.998024	0.000010
6	2	3	0.807977	0.996889	0.999927	0.000012	0.998366		0.000010	0.999981	0.000012
7	3	1	0.000010	0.000010	0.000010	0.000010	0.000010	0.000010		0.000010	0.000010
8	3	2	0.000192	0.993905	1.000000	0.000010	0.998024	0.999981	0.000010		0.000010
9	3	3	0.000010	0.000010	0.000010	0.999969	0.000010	0.000012	0.000010	0.000010	

Figure 16

Region-Position Interaction

Factorial ANOVA of oscillatory % and Region-Position Interaction and Tukey HSD post hoc comparisons. Several pairs of groups were significantly different as depicted by the highlighted values in the post hoc table. Asterisks represent regions that are significantly different from each other at those positions. $F(4, 24041) = 72.677$, $p < 0.01$.

Oscillatory Activity Represented by Cerebellar Lobules

Histological reconstruction of recordings tracks in 2 out of 4 rats was done by aid of electrolytic lesions. For different electrodes in both rats, lesions were made as previously mentioned in the Methods section. As seen in Figure 17, Rat 1 had two lesions from different electrodes, 1 and 3. The lesions produced by electrode 1 and 3 occurred at approximately 3.40 mm and 2.90 mm lateral respectively. In addition, by means of the rat atlas, the electrode 1 lesion was found to be located within Crus 2 whereas the electrode 3 lesion was in the Paramedian Lobule. In Rat 2, the lesion produced by electrode 4 occurred at approximately 3.40 mm lateral. Additionally, this electrode lesion appeared to be situated in the Paramedian Lobule. Table 2 documents the electrode identification and the corresponding coordinates of the electrodes from which lesions were made in each rat, the depth, region and position of the lesion and the associated cerebellar lobule. The depth of each lesion is presented both in turns (raw values of descent of the microelectrode) and corresponding mm measurements. Every turn corresponds to the electrode traveling 0.16 mm. The Region and Position of each lesion is also known since it corresponds to the depth and anteroposterior and mediolateral coordinates of the electrode that produced the lesion respectively. To correctly determine the cerebellar lobule associated with each lesion, histological slides were compared to sagittal images from the rat atlas and identified using lesion depth and anteroposterior/mediolateral coordinates.

Rat 1

1mm

Electrode 1
Lateral 3.40 mm

1mm

Electrode 3
Lateral 2.90 mm

Rat 2

1 mm

Electrode 4
Lateral 3.40 mm

Figure 17

Histological Confirmation of Lesions

Red arrows indicate the electrolytic lesion confirmed histologically. **Rat 1** Left slide: The lesion is located in the Crus 2 Lobule, Right side: The lesion is identified in the Paramedian Lobule. **Rat 2** The lesion is located in the Paramedian Lobule.

Rat	Electrode	Coordinates of Electrode Lesion (mm)	Lesion Depth (turns)	Lesion Depth (mm)	Lesion Region	Lesion Position	Associated Lobule
1	1	Anteroposterior: -13.5 Mediolateral: 4	48	7.68	3	1	Crus 2
	3	Anteroposterior: -11.5 Mediolateral: 2	51	8.16	3	3	Paramedian Lobule
3	4	Anteroposterior: -13.5 Mediolateral: 3	55	8.8	3	1	Paramedian Lobule

Table 2

Electrode Lesions and Histological Confirmation

From left to right columns indicate: (1) Rat identification; (2) Coordinates of the electrode by which the lesion was made; (3) Depth of the lesion in number of turns; (4) Depth of the lesion in millimeters; (5) Corresponding region of lesion based on the depth it was made at; (6) Corresponding position of lesion based on the coordinates of the electrode that made it; (7) Lobule in which the lesion was identified.

As highlighted in table 3, there is a tendency of region 1 being associated with Lobulus Simplex or Crus 1 whereas region 3 usually represents Crus 2 and the Paramedian Lobule. In addition, some regions are composed of different proportions of two associated lobules. The associated lobules that contain an asterisk in Table 3 represent results that were histologically confirmed through a lesion.

Rat	Position	Region	Recording track limits (turns)	Recording track length (mm)	Associated Lobule
1	1	1	8.25 to 21.83	2.17	Lobulus Simplex
		2	21.84 to 35.42	2.17	Crus 1
		3	35.43 to 48.99	2.17	Crus 2 *
	2	1	8.25 to 21.83	2.17	Lobulus Simplex
		2	21.84 to 35.42	2.17	Some Lobulus Simplex/Crus 1
		3	35.43 to 48.99	2.17	Crus 2
	3	1	8.25 to 21.83	2.17	Some Crus 1/Crus 2
		2	21.84 to 35.42	2.17	Crus 2
		3	35.43 to 48.99	2.17	Paramedian Lobule *
3	1	1	10 to 25	2.4	Crus 1
		2	25.01 to 40	2.4	Crus 2
		3	40.01 to 55	2.4	Paramedian Lobule *
	2	1	10 to 25	2.4	Lobulus Simplex
		2	25.01 to 40	2.4	Crus 1
		3	40.01 to 55	2.4	Crus 2

Table 3

Associated Lobules to Positions and Regions

From left to right columns indicate: (1) Rat identification; (2) Position of recording electrode; (3) Region of recording electrode; (4) The interval of turns that constitute the limit of each region; (5) The length of the recording track that constitutes each region; (6) The associated lobule that characterizes each region based on its length. *Asterisks denote associated lobules that were identified histologically by electrolytic lesions.

After associating each region at all positions with a cerebellar lobule, a one-way ANOVA was conducted to determine which, if any, of the four lobules identified had increased oscillatory activity. It is demonstrated in Figure 18 that the Paramedian lobule has increased oscillatory activity that is significantly different from all other lobules; $F(3, 15635) = 113.59$, $p < 0.01$. In addition, the most oscillatory activity is present in the Paramedian Lobule whereas the least rhythmic activity occurs in the Lobulus Simplex. The Tukey HSD post hoc test shows that only the Paramedian lobule is significantly different from the other lobules at $p < 0.01$.

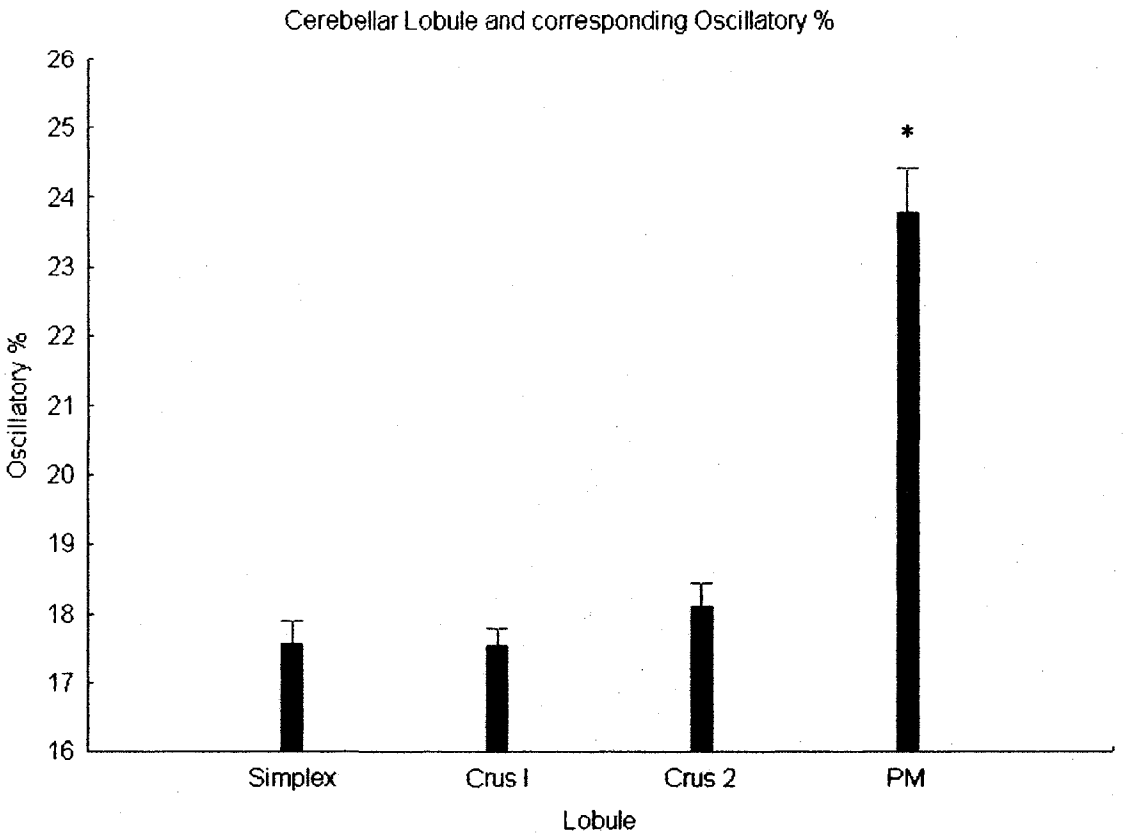

Cell No.	Lobule	{1} 17.553	{2} 17.536	{3} 18.113	{4} 23.780
		Tukey HSD test; variable Oscillatory % Approximate Probabilities for Post Hoc Tests Error: Between MS = 114.69, df = 15635.			
1	Simplex		0.999836	0.097239	0.000008
2	Crus I	0.999836		0.030709	0.000008
3	Crus 2	0.097239	0.030709		0.000008
4	PM	0.000008	0.000008	0.000008	

Figure 18

Cerebellar Lobules and Corresponding Oscillatory Activity

One-way ANOVA of oscillatory % in different cerebellar lobules and Tukey HSD post hoc comparisons. The Paramedian Lobule (PM) is significantly different from all other lobules. $F(3, 15635) = 113.59$, $p < 0.01$.

Discussion

Presence of Oscillations and Histology

The present study is the first to extensively map the location of 5-10 Hz oscillations in the rat cerebellar cortex. We confirm that oscillations in the 5–10 Hz range do occur in the Crus II, as described by Hartmaan and Bower (1998), and add that the paramedian lobule is the site of greatest 5-10 Hz oscillations in the cerebellar granule cell layer of the rat (Figure 8). This study is thus the first to extensively map the oscillatory properties of the rat cerebellar cortex granule cell layer, and did so using multiple moveable microelectrodes. Oscillations were found to occur during valid recording periods and states of immobility in the rat. In addition, recording tracks were reconstructed with the use of post-experiment electrolytic lesions and identified to be anatomically related to lobules XII to XIII and their hemispheric extensions (Crus 1, Crus 2, Paramedian Lobule) depending on the specific target in the implantation site as verified through histological procedures.

Oscillatory activity profile of microelectrodes

As seen is Figure 9, recordings from microelectrodes in the same needle are indeed quite similar and not significantly different from each other. This suggests that even though tips of microelectrodes are not at the exact same location, they are still recording similar field potentials. At the same depth and in the same needle, Figure 10 A, there is a high correlation of both electrodes and oscillatory %. This suggests that different microelectrodes recording a similar site have spectral profiles that are similar. However, recordings from microelectrodes in the same needle at different depths, Figure

10 B, show a slightly different profile, and a much lower correlation. This suggests that depth is a determinant of the strength of rhythmic activity in the 5 – 10 Hz range in the cerebellar granule cell layer. In addition, recordings from microelectrodes at the same depth but in different needles, Figure 10 C, reflecting a difference in mediolateral and/or anteroposterior location, showed the lowest correlation of both electrodes and oscillatory %. Our results point clearly to an effect of electrode location on oscillatory activity. Possible explanations on the effect of depth and location are discussed in the following sections with a detailed analysis of afferent input. It is important to note that the abundance or lack of a specific afferent type or combination of afferents may not be the sole explanation for increased or decreased rhythmic activity. Zonal divisions and compartmentation (Herrup & Kuemerle, 1997) could represent an underlying organizing influence on cerebellar cortex networks.

Oscillatory Activity, Depth, Region, Location and Position

Rhythmic activity in the 5-10 Hz range was correlated with depth in our results. As seen in Figure 11, increased oscillatory activity was more prominent as depth increased in the cerebellum. In addition, Figure 14 demonstrates that the division of depths into one of three regions based on the relative depth of the recording microelectrode in reference to the whole track showed similar results. Oscillatory activity increased from Region 1 to 3. The advantage of using Region as a categorical variable is to parameterize the continuous variable depth.

In addition to depth and region, rhythmic activity in the 5-10 Hz range occurred at distinct locations; Figures 12 and 13 depict increased oscillatory activity at more posterior and lateral locations. Locations at approximately -12.5 mm and -13.5 mm posterior showed increased oscillatory activity and locations in between, and including, coordinates at approximately 2mm and 4mm lateral had increased oscillatory activity. In addition, Figure 15 shows the one-way ANOVA results of classification of anterior-posterior and medial-lateral location to position. It can be seen that increased oscillatory activity was more prominent at Position 1 (lateral caudal, AP: -12.5 to -13.5 mm, ML: 3 to 4 mm) followed by Position 3 (medial rostral, AP: -11.5 mm, ML: 1.5 to 2 mm). Position 2 (lateral rostral, AP: -11.5mm, ML: 3 to 4mm) showed very low levels of oscillatory activity.

The following results could be in part due to distributed afferent input to the cerebellum. As previously mentioned, at the vermis and slightly laterally, there is a concentric distribution of mossy fiber input with vestibular fibers terminating in the base of the fissures, pontocerebellar fibers terminate in the apex of the lobules and spinocerebellar fibers terminate at locations in between (Glickstein, 2000; Voogd & Glickstein, 1998). It may be possible that the results obtained in relation to oscillatory activity and depth/region are due to the different distribution of afferent input. More specifically, afferent input terminates in Crus II and what is considered the hemispheric extensions of lobules VIIB and VIII, namely the Paramedian Lobule (Ramnani, 2006). In this study, histology confirmed that Region 3 is associated with the Crus 2 and Paramedian lobules. Therefore, the increased oscillatory activity that is observed in

Region 3 may be in part due to these afferents. Lateral Crus 2 receives input from prefrontal cortex, motor cortex sends projections to the Paramedian Lobule and the lateral parts of the cerebellum receive a tremendous amount of input from the pons and visual input from visual and motor control centers (Cerminara, Edge, Marple-Horvat, & Apps, 2005; Ramnani, 2006; Voogd & Glickstein, 1998). In addition, pontocerebellar mossy fibers and olivocerebellar projections terminate in the posterior cerebellum; the Paramedian Lobule and Crus 2 receive projections from the pontine nuclei and inferior olive respectively (Voogd, 1991). This distributed afferent input to these areas of the cerebellum may explain the increased oscillatory activity that was observed at more lateral and posterior locations.

Mapping studies of the tactile representation of the granular layer show an intricate organization of peripheral projections; this "fractured somatotopy" is characterized by sites that are activated by a particular input whereas adjacent sites may receive information from distant body parts (Ghez, 1991; Ozol & Hawkes, 1997). Indeed it may be possible that different combinations of afferent input and connectivity in the granular cell layer could be a cause of increased oscillatory activity in the 5-10 Hz range.

Oscillatory Activity and Region-Position Interaction

There is a striking interaction between cerebellar region and position for rhythmic activity in the 5-10 Hz range. It is interesting to note that results show a significant difference between all regions at Position 1 and 3, lateral caudal and medial rostral respectively, with Region 3 consistently providing increased oscillatory activity. It is

thus evident that zonal organization, compartments and afferents could all be a cause of these results seen in this mapping study. In addition, the complexity of the granule layer circuitry (Ito, 2006) along with the cortex's extensive folding and convolutions (Voogd & Glickstein, 1998) adds to the difficulty of functionally mapping its entirety. The decreased amount of rhythmic activity recorded at position 2 may be explained in part due to its overall anterior and lateral coordinates. This position receives less abundant afferent input, in relation to positions 1 and 3, due to the increased proportion of white matter extending to the surface at the junction of lobules VI and VII and lobulus simplex and Crus 1/Crus 2 (Voogd, 1991).

Oscillatory Activity Represented by Cerebellar Lobules

As shown in Figure 17, histological confirmation of electrolytic lesions situates them in the Crus 2 and Paramedian Lobule for 2 rats. Additionally, Table 2 identifies aspects of each lesion such as its depth in turns and millimeters and corresponding region and position. In order to determine which lobule had increased rhythmic activity, each position and region in both rats was associated to a cerebellar lobule as documented in Table 3. In both rats, one of four lobules were identified, the Lobulus Simplex, Crus 1, Crus 2 and Paramedian Lobule. Figure 18 demonstrates that the Paramedian lobule has increased rhythmic activity that is significantly different from all other lobules. In addition, the least rhythmic activity occurs in the Lobulus Simplex and the most oscillatory activity is present in the Paramedian Lobule. In the cerebellum, mossy fibers terminate in patterns that are lobule-specific patches; pontocerebellar fibers terminate in the apex of all lobules and spinocerebellar fibers terminate as a layer just below (Voogd

& Glickstein, 1998). However, the Paramedian Lobule receives an extensive amount of spinocerebellar fiber terminals that is characterized by a very large and distributed area as compared to all other lobules (Voogd & Glickstein, 1998). This increased amount of spinocerebellar afferent input to the paramedian lobule may explain the increased oscillatory activity demonstrated in this study. As mentioned previously, these afferent projections are involved in the planning and initiation of movement and controlling ongoing execution of limb movements (Ghez, 1991). Therefore, these 5-10 Hz oscillations recorded during states of immobility may be a phenomenon implicated in preparing the system prior to the execution of movements and act as a baseline when the system is not overwhelmed with sensory information.

Limitations and Considerations

Whisker movements in rats result in oscillations that occur at a similar frequency from those recorded in the granule cell layer of the immobile rat, therefore it has been speculated that rhythmic activity in the cerebellar cortex may be simply an internal model for whisking (Carvell & Simons, 1990; Nicolelis, Baccala, Lin, & Chapin, 1995). Recent reports show that cerebellar LFP oscillations were present when whisking was null or minimal (O'Connor, Berg, & Kleinfeld, 2002). While whisking was not explicitly controlled in our experiments, it is unlikely to be the whole story. It was also observed in the present experiments that rats in an immobile behavioral state whisked during both oscillatory and non-oscillatory recordings. However, recording periods containing whisking were considered valid since we did not control for whisker movement and rats remained in an immobile state.

The following study does in fact reveal the results of mapping 5-10 Hz oscillations that occur throughout the granule cell layer of the cerebellar cortex. To gain a better understanding of the localization of increased oscillatory activity and make assumptions on the structural architecture that promote this phenomenon a larger mapping area and more recording sites is needed. Specifically, the goal would be to place a large number of electrodes in a small amount of tissue without inducing any significant tissue damage (Buzsaki, 2004; Nadasdy, 1998). Silicone probes have the advantage that they are small, minimize tissue injury and multiple recordings sites could be arranged over a large distance and thus recordings could be made from various layers (Buzsaki, 2004). However, these probes are most advantageous for recording of a superficial surface "matrix", such as in layer V of the somatosensory cortex, as they have an overall shank depth of about 1-1.5 mm (Bartho et al., 2004; Buzsaki, 2004). In this experiment, recordings are made from depths of about 8mm in the cerebellum and therefore silicone probes would be ineffective for mapping. Ideally, our head stages for individual rats would be composed of 4 needles at different positions, each housing 2 microelectrodes and thus allowing recording from 8 microelectrodes at various depths.

Significance

The functional role of the cerebellum characterizes its specific involvement in the pathology of autism. Autism is a disorder which is marked by problems with attention and abnormal responses to sensory stimuli and the environment (Kern, 2002). One area of the brain that has consistently been found to be abnormal in autism is the cerebellum (Kern, 2002). Structural differences such as a reduction of 35-90% in Purkinje cell

number are characteristic of autism (Courchesne, 1997). In addition, regions within the vermis are reduced in area and cerebellar white matter volume may increase up to 40% in autism (Courchesne, 1997). A study by Allen et al. (2004) using fMRI showed that increased regional activation was correlated with the degree of cerebellar structural abnormality. Cerebellar structural abnormalities in autism suggest dysfunction of the cerebellar networks (Allen, Muller, & Courchesne, 2004). In addition to structural differences in cerebellar anatomy, autism is characterized functionally by deficits in sensory and cognitive functions, attention, speech and language (Courchesne, 1997). However, the etiology of autism is poorly understood functionally at the cellular and molecular level to provide explanations for the influence of structural abnormalities at the level of behavior and cognition (Polleux & Lauder, 2004). Neurophysiology may provide an understanding of the effects of the abnormalities in autism on the function of the cerebellar cortex network since multiple neurotransmitter systems may be abnormal in this disorder (Polleux & Lauder, 2004). Hence, a better understanding of cerebellar processing at the circuits level, perhaps through LFP recordings, is necessary for understanding the correlation between structural defects in autism and its influence on components of behavior.

Concluding remarks and future perspectives

As the present study shows, distinct positions and regions in the cerebellum show increased rhythmic 5-10 Hz activity. It is possible that zonal organization, compartments and different combinations of afferent input and connectivity in the granular cell layer could be a cause of increased oscillatory activity in the 5-10 Hz range. This is evident

through the lobule analysis performed; pontocerebellar and large amounts of spinocerebellar afferents both terminate in the cerebellar lobule characterized by the most oscillatory activity, the Paramedian Lobule. In addition, these oscillations in the granule cell layer may be instrumental in preparing the system prior to the execution of movement (De Zeeuw et al., 2008).

To remove the ambiguity of whisker oscillations contaminating the recorded signal it is proposed that video recordings be used to monitor any deflections in vibrissa. A more reliable, but more tedious, means to control for whisker movement is the cutting of afferents to the vibrissae. In the same context, verifying the animal's level of immobility with the use of EMG would be advantageous so that even slight twitches or unobservable movement would be detected.

In this study, LFP microelectrode techniques have been used to gain a more comprehensive functional map of the cerebellar cortex granule cell layer. Future research combining physiological mapping and afferent input tracing methods would confirm present results obtained.

References

Allen, G., Buxton, R. B., Wong, E. C., & Courchesne, E. (1997). Attentional activation of the cerebellum independent of motor involvement. *Science, 275*(5308), 1940-1943.

Allen, G., Muller, R. A., & Courchesne, E. (2004). Cerebellar function in autism: functional magnetic resonance image activation during a simple motor task. *Biol Psychiatry, 56*(4), 269-278.

Apps, R., & Garwicz, M. (2005). Anatomical and physiological foundations of cerebellar information processing. *Nat Rev Neurosci, 6*(4), 297-311.

Armstrong, C. L., & Hawkes, R. (2000). Pattern formation in the cerebellar cortex. *Biochem Cell Biol, 78*(5), 551-562.

Baker, S. N., Kilner, J. M., Pinches, E. M., & Lemon, R. N. (1999). The role of synchrony and oscillations in the motor output. *Exp Brain Res, 128*(1-2), 109-117.

Bartho, P., Hirase, H., Monconduit, L., Zugaro, M., Harris, K. D., & Buzsaki, G. (2004). Characterization of neocortical principal cells and interneurons by network interactions and extracellular features. *J Neurophysiol, 92*(1), 600-608.

Bear, M. F., Connors, Barry W., Paradiso, Michael A. (2001). *Neuroscience: Exploring the Brain* (Second ed.). Baltimore: Lippincott Williams and Wilkins.

Bedard, C., Kroger, H., & Destexhe, A. (2004). Modeling extracellular field potentials and the frequency-filtering properties of extracellular space. *Biophys J, 86*(3), 1829-1842.

Bellebaum, C., & Daum, I. (2007). Cerebellar involvement in executive control. *Cerebellum, 6*(3), 184-192.

Borisyuk, R., & Kazanovich, Y. (2006). Oscillations and waves in the models of interactive neural populations. *Biosystems, 86*(1-3), 53-62.

Bower, J. M. (2002). The organization of cerebellar cortical circuitry revisited: implications for function. *Ann N Y Acad Sci, 978*, 135-155.

Buzsaki, G. (2002). Theta oscillations in the hippocampus. *Neuron, 33*(3), 325-340.

Buzsaki, G. (2004). Large-scale recording of neuronal ensembles. *Nat Neurosci, 7*(5), 446-451.

Buzsaki, G. (2006). *Rhythms of the Brain.* New York: Oxford University Press.

Buzsaki, G., & Draguhn, A. (2004). Neuronal oscillations in cortical networks. *Science, 304*(5679), 1926-1929.

Carvell, G. E., & Simons, D. J. (1990). Biometric analyses of vibrissal tactile discrimination in the rat. *J Neurosci, 10*(8), 2638-2648.

Cerminara, N. L., Edge, A. L., Marple-Horvat, D. E., & Apps, R. (2005). The lateral cerebellum and visuomotor control. *Prog Brain Res, 148*, 213-226.

Chen, Y., Nitz, D.A. (2003). Evidence for slow (2–10 Hz) and gamma frequency coherence between spike trains and local field potentials in the cerebellum. *Neurocomputing, 52-54*, 159-164.

Cooper, J. R., Bloom, F.E. and Roth, R.H. . (2003). *The Biochemical Basis of Neuropharmacology*. New York: Oxford University Press.

Courchesne, E. (1997). Brainstem, cerebellar and limbic neuroanatomical abnormalities in autism. *Curr Opin Neurobiol, 7*(2), 269-278.

Courtemanche, R., & Lamarre, Y. (2005). Local field potential oscillations in primate cerebellar cortex: synchronization with cerebral cortex during active and passive expectancy. *J Neurophysiol, 93*(4), 2039-2052.

Courtemanche, R., Pellerin, J. P., & Lamarre, Y. (2002). Local field potential oscillations in primate cerebellar cortex: modulation during active and passive expectancy. *J Neurophysiol, 88*(2), 771-782.

D'Angelo, E., Nieus, T., Maffei, A., Armano, S., Rossi, P., Taglietti, V., et al. (2001). Theta-frequency bursting and resonance in cerebellar granule cells: experimental evidence and modeling of a slow k+-dependent mechanism. *J Neurosci, 21*(3), 759-770.

De Schutter, E., & Bjaalie, J. G. (2001). Coding in the granular layer of the cerebellum. *Prog Brain Res, 130*, 279-296.

De Zeeuw, C. I., Hoebeek, F. E., & Schonewille, M. (2008). Causes and consequences of oscillations in the cerebellar cortex. *Neuron, 58*(5), 655-658.

Devor, A. (2002). The great gate: control of sensory information flow to the cerebellum. *Cerebellum, 1*(1), 27-34.

Dieudonne, S., & Dumoulin, A. (2000). Serotonin-driven long-range inhibitory connections in the cerebellar cortex. *J Neurosci, 20*(5), 1837-1848.

Ermentrout, G. B., Chow, C. C. (2002). Modeling neural oscillations. *Physiol Behav, 77*(4-5), 629-633.

Forti, L., Cesana, E., Mapelli, J., & D'Angelo, E. (2006). Ionic mechanisms of autorhythmic firing in rat cerebellar Golgi cells. *J Physiol, 574*(Pt 3), 711-729.

Geurts, F. J., De Schutter, E., & Dieudonne, S. (2003). Unraveling the cerebellar cortex: cytology and cellular physiology of large-sized interneurons in the granular layer. *Cerebellum, 2*(4), 290-299.

Ghez, C. (1991). The Cerebellum. In *Principles of Neural Science* (pp. 626-646). New York: Elsevier Science Publishing Co. Inc.

Glickstein, M. (2000). Functional localisation in the cerebral cortex and cerebellum: lessons from the past. *Eur J Morphol, 38*(5), 291-300.

Gomi, H., & Kawato, M. (1992). Adaptive feedback control models of the vestibulocerebellum and spinocerebellum. *Biol Cybern, 68*(2), 105-114.

Gordon, N. (2007). The cerebellum and cognition. *Eur J Paediatr Neurol, 11*(4), 232-234.

Gray, C. M. (1994). Synchronous oscillations in neuronal systems: mechanisms and functions. *J Comput Neurosci, 1*(1-2), 11-38.

Gray, C. M., & Singer, W. (1989). Stimulus-specific neuronal oscillations in orientation columns of cat visual cortex. *Proc Natl Acad Sci U S A, 86*(5), 1698-1702.

Hartmann, M. J., & Bower, J. M. (1998). Oscillatory activity in the cerebellar hemispheres of unrestrained rats. *J Neurophysiol, 80*(3), 1598-1604.

Heck, D. H., Thach, W. T., & Keating, J. G. (2007). On-beam synchrony in the cerebellum as the mechanism for the timing and coordination of movement. *Proc Natl Acad Sci U S A, 104*(18), 7658-7663.

Herrup, K., & Kuemerle, B. (1997). The compartmentalization of the cerebellum. *Annu Rev Neurosci, 20*, 61-90.

Ito, M. (1984). *The Cerebellum and Neural Control*. New York: Raven Press.

Ito, M. (2006). Cerebellar circuitry as a neuronal machine. *Prog Neurobiol, 78*(3-5), 272-303.

Jedlicka, P., & Backus, K. H. (2006). Inhibitory transmission, activity-dependent ionic changes and neuronal network oscillations. *Physiol Res, 55*(2), 139-149.

Kelly, R. M., & Strick, P. L. (2003). Cerebellar loops with motor cortex and prefrontal cortex of a nonhuman primate. *J Neurosci, 23*(23), 8432-8444.

Kern, J. K. (2002). The possible role of the cerebellum in autism/PDD: disruption of a multisensory feedback loop. *Med Hypotheses, 59*(3), 255-260.

Labrakakis, C., Muller, T., Schmidt, K., & Kettenmann, H. (1997). GABA(A) receptor activation triggers a Cl- conductance increase and a K+ channel blockade in cerebellar granule cells. *Neuroscience, 79*(1), 177-189.

Lang, E. J., Sugihara, I., Welsh, J. P., & Llinas, R. (1999). Patterns of spontaneous purkinje cell complex spike activity in the awake rat. *J Neurosci, 19*(7), 2728-2739.

Laurent, G. (2002). Olfactory network dynamics and the coding of multidimensional signals. *Nat Rev Neurosci, 3*(11), 884-895.

Leznik, E., & Llinas, R. (2005). Role of gap junctions in synchronized neuronal oscillations in the inferior olive. *J Neurophysiol, 94*(4), 2447-2456.

Llinás, R. R., Walton, K.D, Lang, E.J. . (2004). Cerebellum. In *The Synaptic Organization of the Brain* (Fifth ed., pp. 736). New York: Oxford University Press.

Lu, H., Hartmann, M. J., & Bower, J. M. (2005). Correlations between purkinje cell single-unit activity and simultaneously recorded field potentials in the immediately underlying granule cell layer. *J Neurophysiol, 94*(3), 1849-1860.

Maex, R., & De Schutter, E. (1998). Synchronization of golgi and granule cell firing in a detailed network model of the cerebellar granule cell layer. *J Neurophysiol, 80*(5), 2521-2537.

Maex, R., & De Schutter, E. (2005). Oscillations in the cerebellar cortex: a prediction of their frequency bands. *Prog Brain Res, 148*, 181-188.

Manto, M. U. (2006). On the cerebello-cerebral interactions. *Cerebellum, 5*(4), 286-288.

Mohler, H. (2006). GABA(A) receptor diversity and pharmacology. *Cell Tissue Res, 326*(2), 505-516.

Nadasdy, Z., Csicsvari, J., Penttonen, M., Hetke, J., Wise, K., Buzsaki, G. (1998). Extracellular Recording and Analysis of Neuronal Activity: From Single Cells to Ensembles. In *Neuronal Ensembles: Strategies for Recording and Decoding* (pp. 17-56). New York: Wiley-Liss.

Nakanishi, S. (2005). Synaptic mechanisms of the cerebellar cortical network. *Trends Neurosci, 28*(2), 93-100.

Nicolelis, M. A., Baccala, L. A., Lin, R. C., & Chapin, J. K. (1995). Sensorimotor encoding by synchronous neural ensemble activity at multiple levels of the somatosensory system. *Science, 268*(5215), 1353-1358.

O'Connor, S. M., Berg, R. W., & Kleinfeld, D. (2002). Coherent electrical activity between vibrissa sensory areas of cerebellum and neocortex is enhanced during free whisking. *J Neurophysiol, 87*(4), 2137-2148.

Ozol, K. O., & Hawkes, R. (1997). Compartmentation of the granular layer of the cerebellum. *Histol Histopathol, 12*(1), 171-184.

Paxinos, G., Watson, C. (1998). *The Rat Brain: In Stereotaxic Coordinates* (Forth ed.): Academic Press.

Pellerin, J. P., & Lamarre, Y. (1997). Local field potential oscillations in primate cerebellar cortex during voluntary movement. *J Neurophysiol, 78*(6), 3502-3507.

Polleux, F., & Lauder, J. M. (2004). Toward a developmental neurobiology of autism. *Ment Retard Dev Disabil Res Rev, 10*(4), 303-317.

Ramnani, N. (2006). The primate cortico-cerebellar system: anatomy and function. *Nat Rev Neurosci, 7*(7), 511-522.

Ritz, R., & Sejnowski, T. J. (1997). Synchronous oscillatory activity in sensory systems: new vistas on mechanisms. *Curr Opin Neurobiol, 7*(4), 536-546.

Rossi, D. J., Hamann, M., & Attwell, D. (2003). Multiple modes of GABAergic inhibition of rat cerebellar granule cells. *J Physiol, 548*(Pt 1), 97-110.

Saab, C. Y., & Willis, W. D. (2003). The cerebellum: organization, functions and its role in nociception. *Brain Res Brain Res Rev, 42*(1), 85-95.

Salman, M. S. (2002). The cerebellum: it's about time! But timing is not everything--new insights into the role of the cerebellum in timing motor and cognitive tasks. *J Child Neurol, 17*(1), 1-9.

Sillitoe, R. V., & Joyner, A. L. (2007). Morphology, molecular codes, and circuitry produce the three-dimensional complexity of the cerebellum. *Annu Rev Cell Dev Biol, 23*, 549-577.

Toga, A. W., Mazziotta, J.C. (2002). *Brain Mapping: The Methods*. San Diego: Academic Press.

Voogd, J. (1991). Cerebellum. In *The Rat Nervous System* (Third ed., pp. 205-239). San Diego: Elsevier Academic Press.

Voogd, J. (2003). The human cerebellum. *J Chem Neuroanat, 26*(4), 243-252.

Voogd, J., Gerrits, N. M., & Ruigrok, T. J. (1996). Organization of the vestibulocerebellum. *Ann N Y Acad Sci, 781*, 553-579.

Voogd, J., & Glickstein, M. (1998). The anatomy of the cerebellum. *Trends Neurosci, 21*(9), 370-375.

Vos, B. P., Maex, R., Volny-Luraghi, A., & De Schutter, E. (1999). Parallel fibers synchronize spontaneous activity in cerebellar Golgi cells. *J Neurosci, 19*(11), RC6.

Wang, X. J., & Rinzel, J. (1993). Spindle rhythmicity in the reticularis thalami nucleus: synchronization among mutually inhibitory neurons. *Neuroscience, 53*(4), 899-904.

Welsh, J. P., Lang, E. J., Suglhara, I., & Llinas, R. (1995). Dynamic organization of motor control within the olivocerebellar system. *Nature, 374*(6521), 453-457.